

FOUNDRY PRACTICE

The authoritative magazine for foundry engineers

- SINCE 1932 -



| FILTRATION

Further Evaluating Iron Filter Print Designs

| MOULD & CORE

Reducing Formaldehyde Emissions from Water-Based Coatings

Reclamation of Inorganic Bonded Sand Systems
Towards a More Sustainable Core Production Process

| METALLURGICAL AND POURING CONTROL

An Investment Casting Foundry Experience in Improving
Degassing and Grain Refining in Molten Aluminium Alloys

Melt Quality Investigation for High Integrity Aluminium
Castings

| COATINGS & FEEDING SYSTEMS

Paradigm shift: an Indian Foundry Experience

EDITORIAL

As a company, we have a simple mission: to help our customers improve their operating performance. As the articles in this issue of Foundry Practice demonstrate, it is something we are very good at. But improving innovation and performance brings other benefits: a more efficient and productive process also reduces environmental impacts.

In 2020, we took our environmental responsibility to the next level, launching a new sustainability initiative. Our goal is to create a better tomorrow for our planet, our customers, our people and our communities. Papers that demonstrate specific sustainability benefits are now highlighted with sustainability logos. Look out for them as you read through the issue!

In addition, we are investing even more in innovation to underline our commitment to the industry and aspire to expand our leadership position.



FURTHER EVALUATING IRON FILTER PRINT DESIGNS

A follow-up to a 2017 paper that documented qualitative analyses of filter print designs, this paper presents the results of subsequent quantitative analysis and evaluation of several filter print design concepts using casting process simulation software.

REDUCING FORMALDEHYDE EMISSIONS FROM WATER-BASED COATINGS

With formaldehyde (FH) emission limits tightening in the EU, the release of FH from water-based coatings is under scrutiny. This paper discusses a new generation of FH-free coatings that are designed to help foundries comply with the latest regulatory requirements, without impacting performance.

AN INVESTMENT CASTING FOUNDRY EXPERIENCE IN IMPROVING DEGASSING AND GRAIN REFINING IN MOLTEN ALUMINIUM ALLOYS

Recent technological developments are raising the performance and lowering the environmental impact of aluminium alloy treatment processes. This paper discusses these improvements as implemented at a foundry in New Jersey, USA, with discussion of the pre-implementation rationale and evaluation process, as well as the achieved technical, economic and environmental benefits.

MELT QUALITY INVESTIGATION FOR HIGH INTEGRITY ALUMINIUM CASTINGS

The use of the MTS 1500 process has been demonstrated to improve melt cleanliness in the manufacture of high-integrity aluminium castings. This paper discusses some recent case studies, focusing on high-pressure die casting applications and the use of VMET melt quality assessment to quantify the level of melt quality improvement.

RECLAMATION OF INORGANIC BONDED SAND SYSTEMS TOWARDS A MORE SUSTAINABLE CORE PRODUCTION PROCESS

This paper presents an innovative process for the effective reclamation of foundry sand from cores made with the SOLOSIL* TX inorganic binding system.

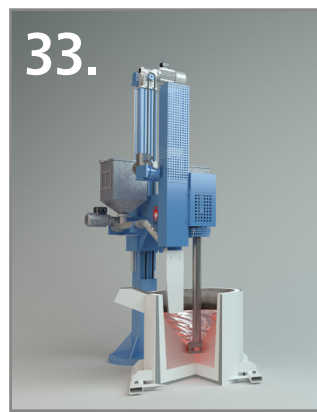
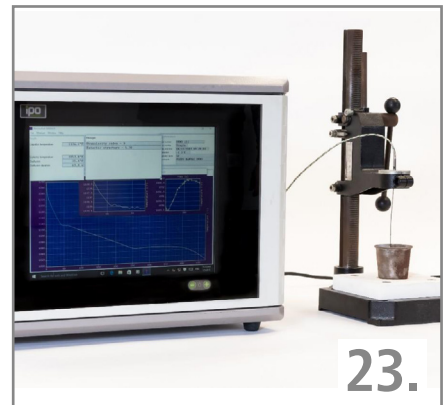
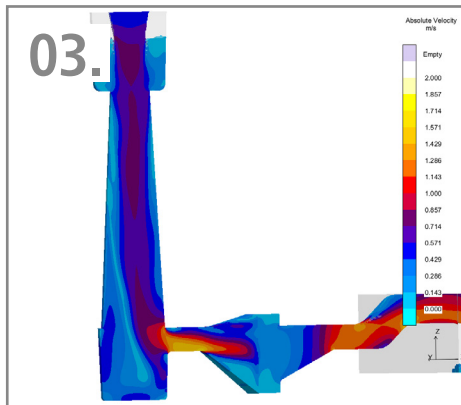
PARADIGM SHIFT: AN INDIAN FOUNDRY EXPERIENCE

Bradken and Foseco have forged a close association in India, working together to create value by improving foundry processes and the development of castings. This paper highlights the outcomes of this joint effort and the benefits of collaboration.

I hope you enjoy reading this edition.

JOHN SUTHERLAND
Intl. Marketing Services Manager

CONTENTS



03. IRON FOUNDRIES FILTRATION

Further Evaluating Iron Filter Print Designs

Author: Tony Midea, Foseco

16. IRON FOUNDRIES COATINGS

Reducing Formaldehyde Emissions from Water-Based Coatings

Authors: Christoph Genzler and Rene Roeleveld, Foseco



23. NON-FERROUS FOUNDRIES METALLURGICAL AND POURING CONTROL

An Investment Casting Foundry Experience In Improving Degassing And Grain Refining In Molten Aluminium Alloys

Authors: Robert Zebick; Atlantic Casting & Engineering and Brian Began; Foseco Foundry Division, Vesuvius PLC

33. NON-FERROUS FOUNDRIES METALLURGICAL AND POURING CONTROL

Melt Quality Investigation For High Integrity Aluminium Castings

Authors: Philippe Kientzler (MSc) and Takehiko Okamoto, Foseco Japan, Tenco Xue, Foseco China and Pramuk Uhapattanapanich, Foseco Thailand

44. IRON FOUNDRIES BINDERS

Reclamation of inorganic bonded sand systems towards a more sustainable core production process

Authors: Dr. Vincent Haanappel and Thomas Linke, Foseco and Markus Jendrock and Dr. Enno Schulte, KLEIN Anlagenbau AG

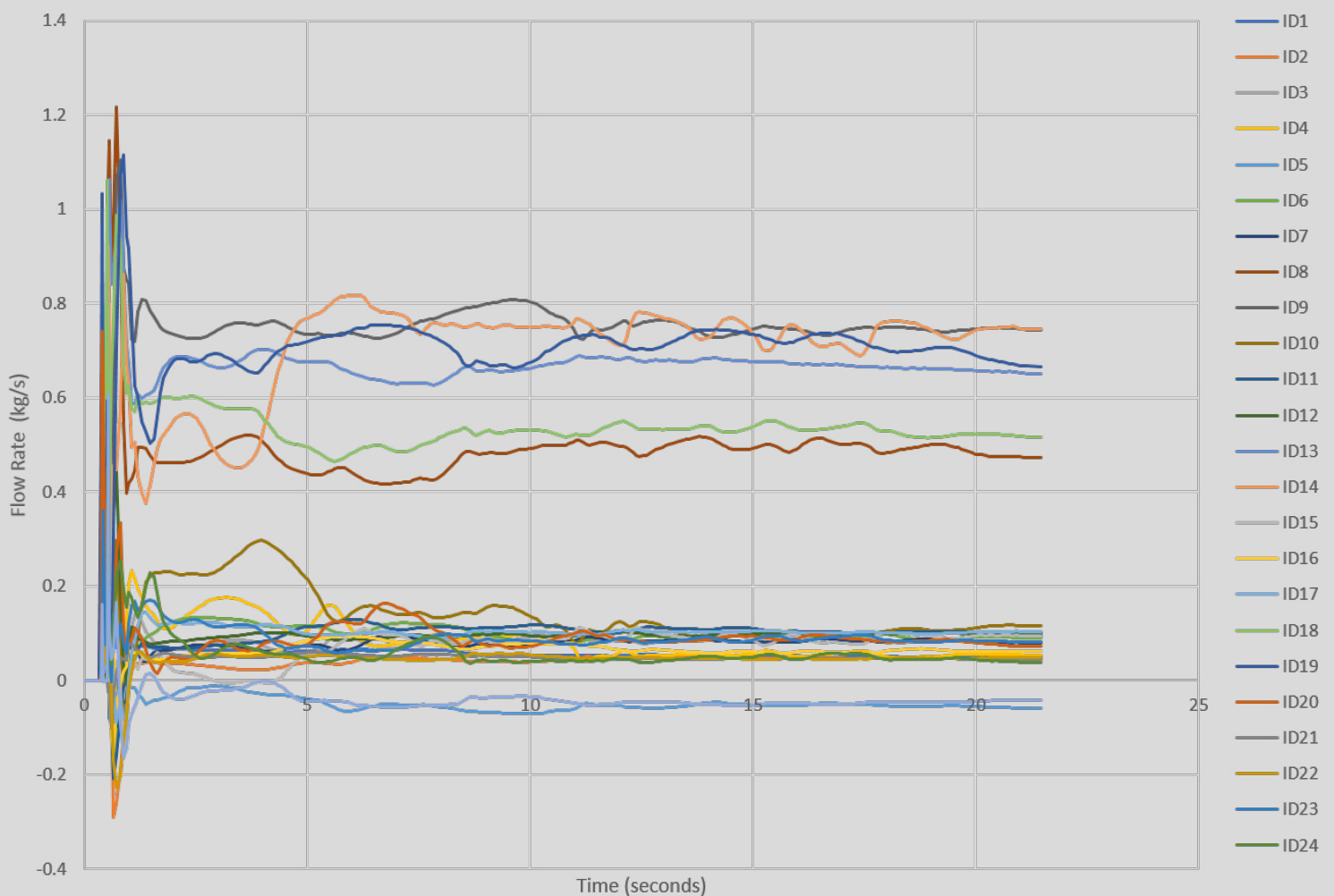


51. IRON FOUNDRIES COATINGS AND FEEDING SYSTEMS

Paradigm shift: an Indian Foundry Experience

Authors: Archis Patankar, Manilal Bhimani and Sondip Bor, Foseco India Limited and Paramasivan Subramanian and Rajkumar B, Bradken India Private Limited





FURTHER EVALUATING IRON FILTER PRINT DESIGNS USING QUANTITATIVE ANALYSES



Author: Tony Midea

Properly filtering iron castings involves utilizing the most optimally engineered filter print and gating system designs to ensure delivery of the cleanest and least turbulent metal to the mold cavity. In 2017, Tony Midea co-wrote a Foundry Practice paper that documented qualitative analyses of filter print designs entitled "Evaluating Iron Filter Print Designs – 30 Years Later"¹. That paper utilized the most advanced fluid flow technology to assess filter print designs fluid flow characteristics, and to recommend best practice application techniques and methodology to the iron foundry industry.

A follow-on study was undertaken to couple quantitative analyses with qualitative analyses to ensure that the best filter print designs were being recommended. Results from the quantitative analyses shown in this paper support the recommendations from 2017 and provide further insight on best practice filter print designs.

INTRODUCTION

This work focuses on analysis and evaluation of several filter print design concepts²⁻¹⁰ using casting process simulation software employing sophisticated, first principle fluid flow analysis models. The goal is to investigate problems experienced in foundries and maximize the benefits of filtration to deliver the best possible quality molten metal to the mold cavity, thereby producing high quality castings.

The first section of this paper will provide a summary review of the work documented in the 2017 paper referenced above. This includes the qualitative analyses that involved evaluating fluid flow characteristics within the filtration system to determine best practice.

The second section of this paper will document the methodology used to define the quantitative analyses and provide a detailed examination of the results from the quantitative analyses. The quantitative and qualitative analyses are combined to recommend best practice filter print designs.

METHOD OF ANALYSIS

Standard 75mm x 75mm x 22mm (2.95x2.95x0.866 inch) thick square vertical filter prints were chosen as the baseline for these analyses. Several modifications were made to the filter prints to evaluate the effect of these design modifications on fluid dynamics.

All fluid flow analyses were conducted using MAGMA5 (Version 5.4.0.4) with Solver 5. The mesh size for all simulations was approximately 10 million elements (700,000 metal cells). The metal dataset represents ASTM A536-84 (80-55-06/GGG-60) grade ductile iron poured at 1400°C (2552°F) into a sand mold. The plate casting is approximately 305x610x76mm (12x24x3in) in dimension and approximately 100kg (220lb) in weight. Total pour weight was approximately 110kg (242lb).

The filters were represented using standard 10, 20 and 30ppi, foam filtration pressure drop data for a 22mm (0.866in) thick filter¹¹. In all cases, the program was run using the "Automatic Filling Control" feature. Specifically, the program was forced to maintain a pouring cup metal height of 70% for all the simulations, thus ensuring identical pouring conditions for all versions simulated. Fill time was approximately 24 seconds for all configurations, representing a flow rate of approximately 4.5kg/s (10lb/s).

The gating designs evaluated in this report are representative of those in use on industry standard, high pressure, green sand, automated molding equipment.

The choke area was calculated using Equation 1.

$$A = \frac{W}{tDC\sqrt{(2gH)}}$$

The top of the sprue was calculated using Equation 2.

$$A_{\text{Sprue Top}} = \frac{V_{\text{PL}} \times A_{\text{PL}}}{V_{\text{ST}}}$$

The sprue was tapered at three degrees to allow for mold stripping.

The runner system follows a ratio of Sprue:Runner:Ingate of 1.0:1.1:1.2. The baseline vertical filter print configuration is shown in Figure 1.

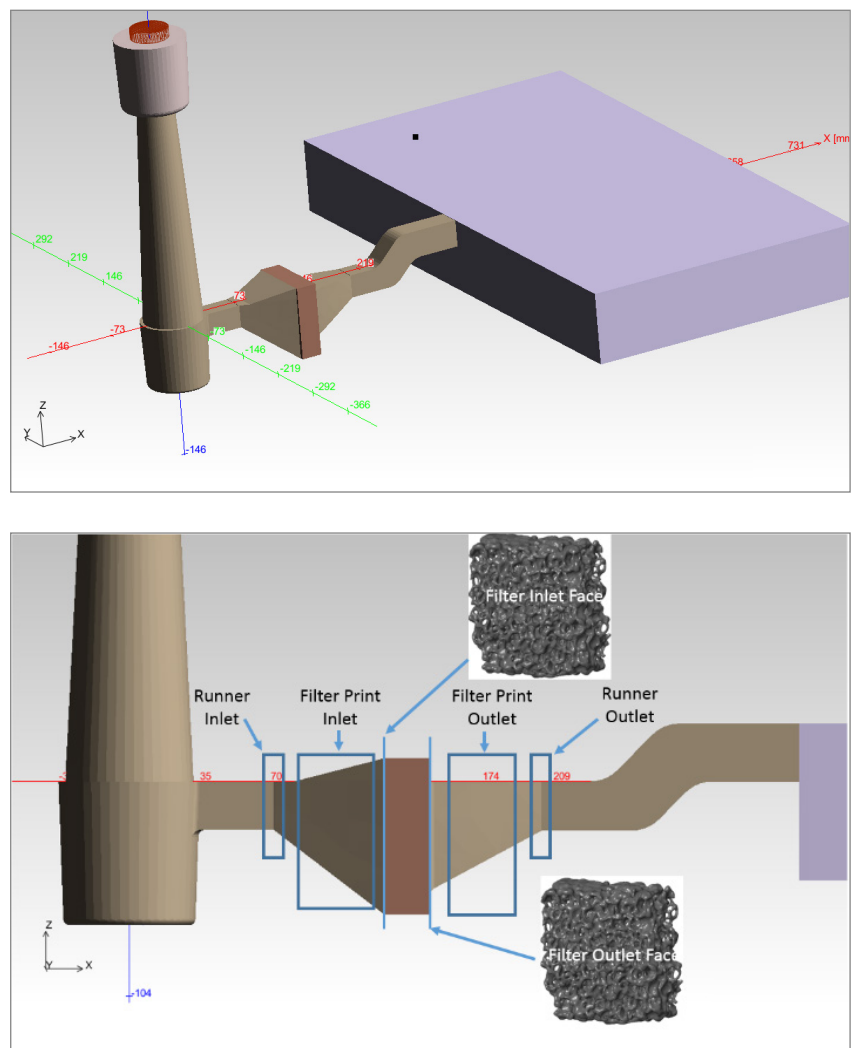


Figure 1. Standard Vertical Filter Print

RESULTS AND DISCUSSION

All fluid flow results shown are analytical and based on the Navier-Stokes flow equations. Flow predictions from this first principal fluid dynamic approach have been validated for several decades in many industries and applications, including molten metal applications. The expectation is that the comparative results shown should be very meaningful and accurate.

QUALITATIVE ANALYSES – SUMMARY REVIEW OF 2017 VERTICAL FILTER PRINT RESULTS

The flow characteristics for a standard vertical filter print are shown in Figure 2. The colors represent flow velocities.

At 10% filled, the flow is steady state in and around the filter print. The color scale ranges from light blue (low velocity, near 0.2 m/s (0.66 ft/s)) to white (higher velocity, near 2.0 m/s (6.6 ft/s)). Flow through the filter is approximately 0.3-0.4 m/s (1-1.3 ft/s), and the flow before the filter is laminar, and covers the entire filter. Flow after the filter is uniform and stable.

A cross section through the middle of the filter print at this same time step shows the fluid velocity and flow vectors (Figure 3).

This image clearly shows the uniform flow, and the utilization of the entire filter face for both flow control and filtration. This can be considered a well-designed filter print and gating system that serves as a baseline for this section of the paper.

In application, extreme changes have sometimes been made to standard filter prints to save weight, increase yield and/or fit within pattern plate restrictions. Figure 4 shows one actual example.

While this design results in a 35% weight reduction to the filter print design (0.9kgs, 2lbs), the flow characteristics in the filter print and gating system are adversely affected.

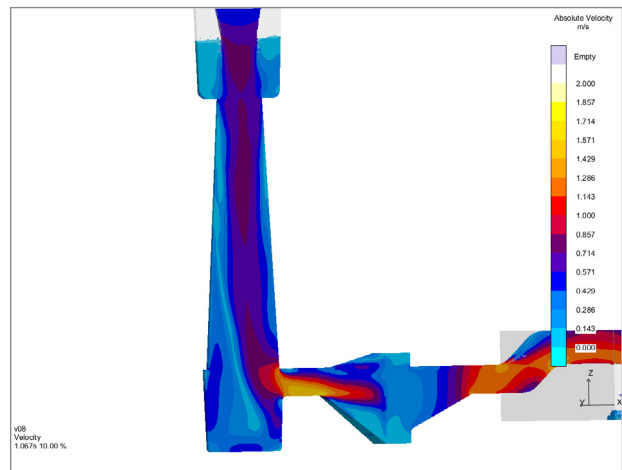


Figure 2. Centerline Cross-Section of Standard Vertical Filter Print Gating System Flow Velocity at 10% Filled

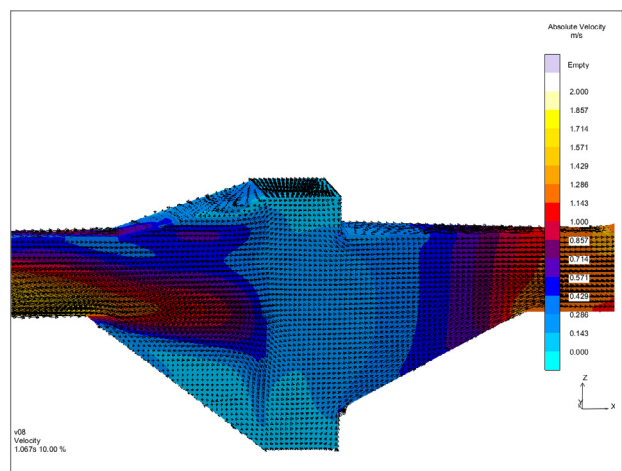


Figure 3. Centerline Cross-Section of Standard Vertical Filter Print Flow Velocity at 10% Filled

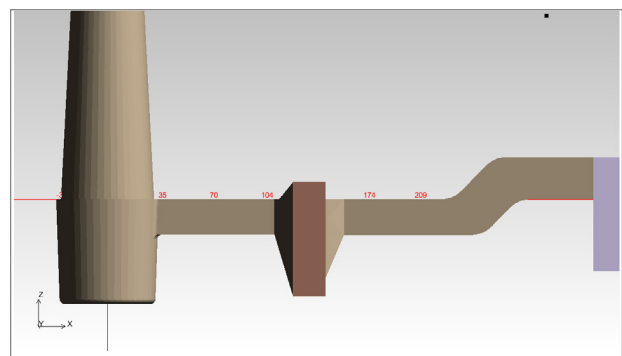


Figure 4. Vertical Filter Print with Filter Print Inlet and Outlet Areas Significantly Reduced

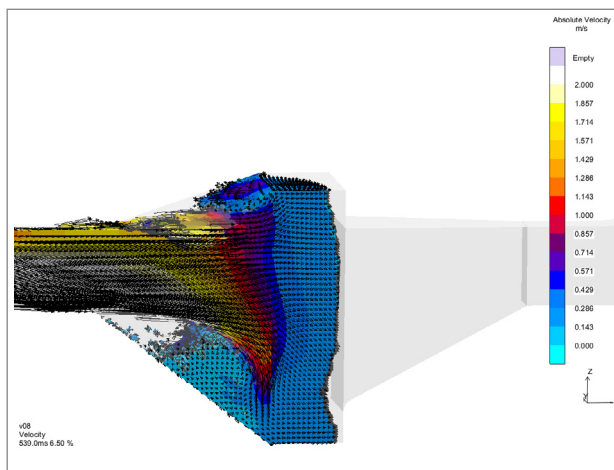
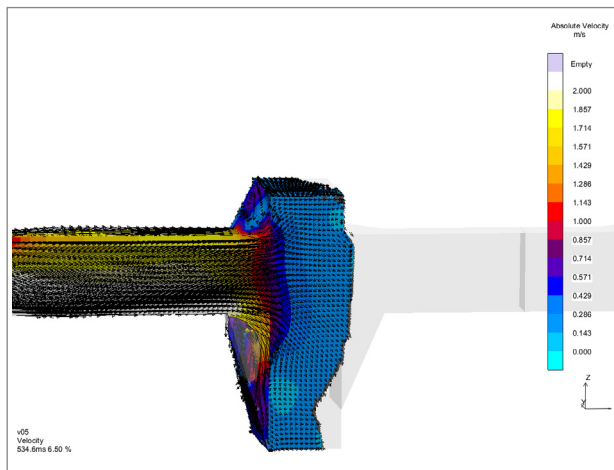


Figure 5. Flow Comparison for Vertical Filter Print with Filter Print Inlet and Outlet Areas Significantly Reduced at 6.5% Filled

Figure 5 shows the flow characteristics at the centerline of the filter print and gating system at 6.5% filled.

(Note: The results for all designs are compared to the standard filter print design results. The standard results are shown as the bottom image in the comparative figures for the vertical filter print examples).

Because of the sharp angles of the modified filter print inlet, the flow accelerates into the center of the filter inlet face and begins to move through the filter before completely filling up the filter print inlet area. The flow characteristics for the standard filter print design show a more evenly distributed flow pattern within the filter print inlet and at the filter inlet face.

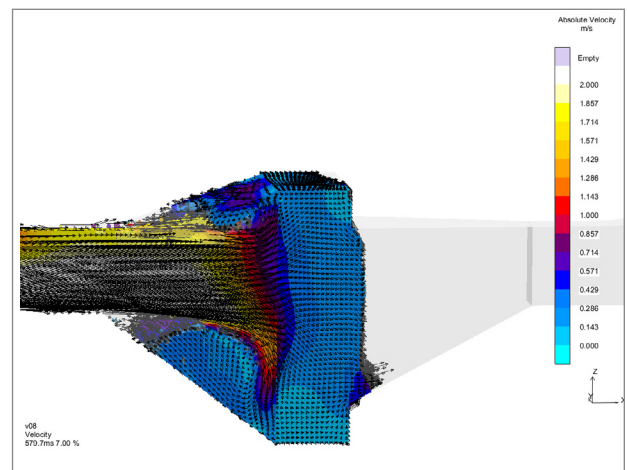
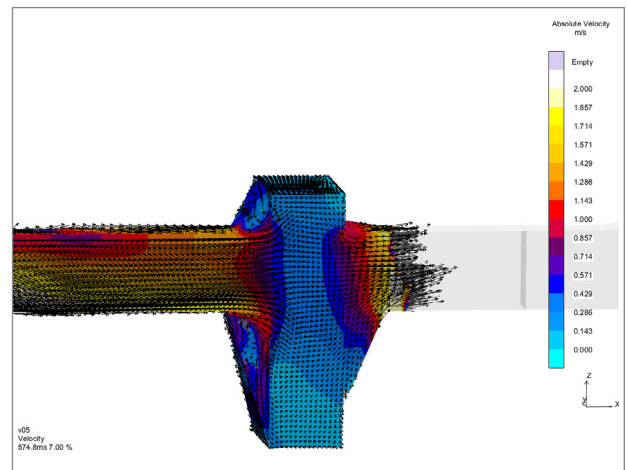


Figure 6. Flow Comparison for Vertical Filter Print with Filter Print Inlet and Outlet Areas Significantly Reduced at 7.0% Filled

The high filter inlet face velocities of the reduced filter print inlet area design results in some very high filter exit face velocities, as shown in Figure 6.

Ideally, the filter should reduce flow energy and turbulence by acting as a flow discontinuity. However, this effect is mitigated if only a small area of the filter is being utilized. This is shown clearly in Figure 6, with the reduced area filter print showing flow exiting the filter at high velocity, while the standard design shows the entire filter filled with metal at very low velocity, and minimal metal flow exiting the filter itself at this time step.

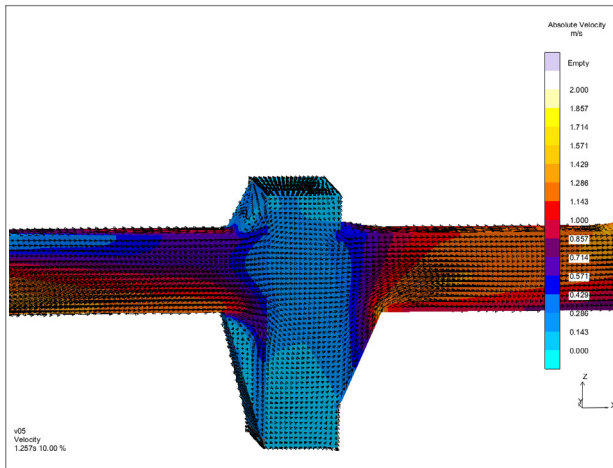


Figure 7. Flow Comparison for Vertical Filter Print with Filter Print Inlet and Outlet Areas Significantly Reduced at 10.0% Filled

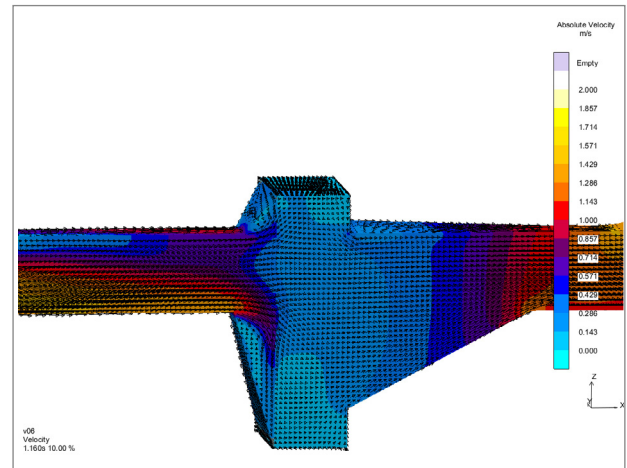


Figure 9. Flow Comparison for Vertical Filter Print with Filter Print Inlet Area Significantly Reduced at 10.0% Filled

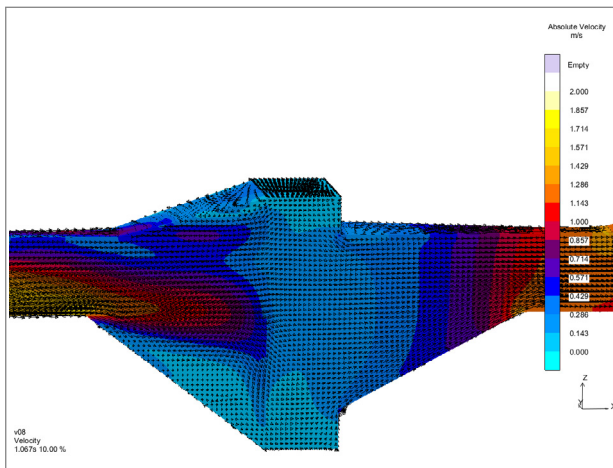


Figure 8. Vertical Filter Print with Filter Print Inlet Area Significantly Reduced

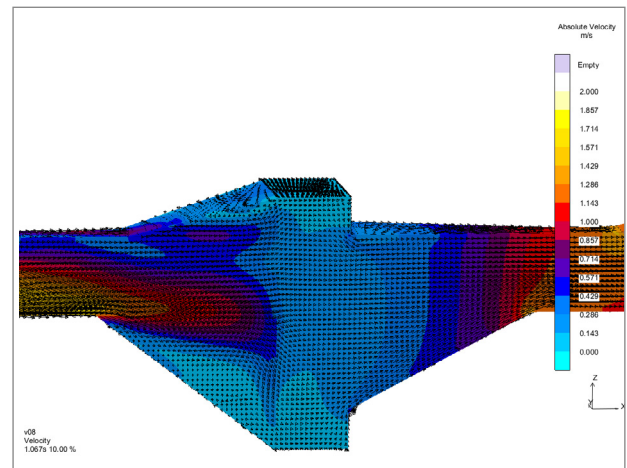


Figure 8. Vertical Filter Print with Filter Print Inlet Area Significantly Reduced

In Figure 7, this continues to be the case even at steady state flow.

Even at steady state, the reduced area filter print design is not allowing the entire filter print inlet area to be used, and instead is pushing the metal through the center of the filter. This results in non-uniform flow behind the filter, and the potential for turbulence. Contrast this with the uniform flow profile shown for the standard filter print design, particularly at the filter outlet face, the filter print outlet and downstream in the runner.

Reducing the area of the filter print in this fashion to slightly increase yield (0.9kg, 2lbs saved) has significant adverse effects on the flow characteristics in the filter print inlet, the filter inlet face, the filter outlet face, the filter print outlet, and in the downstream runner bar. This type of alteration is not recommended for best practice filter print design.

Figure 8 shows a configuration with the area of the filter print outlet modified to match the standard print shown in Figure 1, but the reduced filter print inlet area is unchanged.

In this case, the issues in the filter print inlet area and at the filter inlet face remain the same as discussed previously, but the flow after the filter shows clear improvement. In Figure 9, note how similar the filter outlet face and filter print outlet flow profiles appear when comparing the reduced filter print inlet area configuration with the standard filter print.

The main difference between this configuration and the standard filter print is the dramatically higher flow velocities at the filter inlet face for the reduced area design, and the fact that only a small portion of the filter is being used. This is the same situation discussed in the previous configuration, but the yield argument is even more clear this time.

Reducing the area of the filter print inlet only saves 0.6kg (1.3lb), but adversely affects the flow such that the entire filter area is not being used to efficiently filter inclusions from the metal. Again, this small yield improvement has a significant adverse effect on the flow and is not recommended in practice.

Figure 10 shows a similar design with the area reduced at the filter print outlet only.

Reducing the area of the filter print outlet only will save just 0.3kg (0.66lb), and results in very poor flow exiting the filter print. The flow comparison is shown in Figure 11.

In this case, the flow in the filter print inlet and at the filter inlet face has the same beneficial characteristics as that of the standard filter print. However, the flow at the filter outlet face, within the filter print outlet and in the downstream runner bar exhibits the same poor characteristics shown in Figures 5-7. A filter print design that adversely affects the flow characteristics and delivers minimal yield improvement should not be considered as practical.

Figure 12 shows the standard configuration with an addition of a slag trap before the filter.

This change only adds approximately 0.23kgs (0.5lbs) to the filter print design, but results in a positive impact on the overall flow characteristics of the filter print itself.

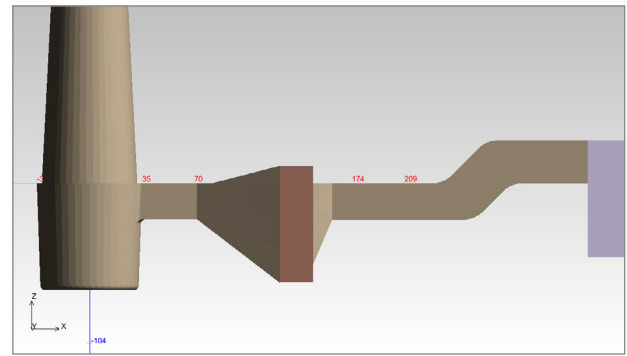


Figure 10. Vertical Filter Print with Filter Print Outlet Area Significantly Reduced

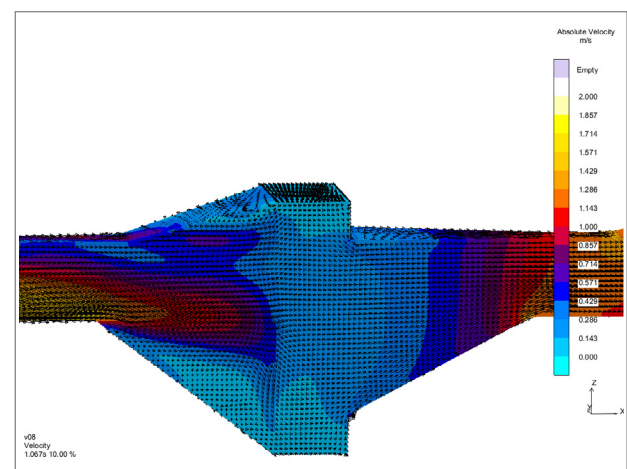
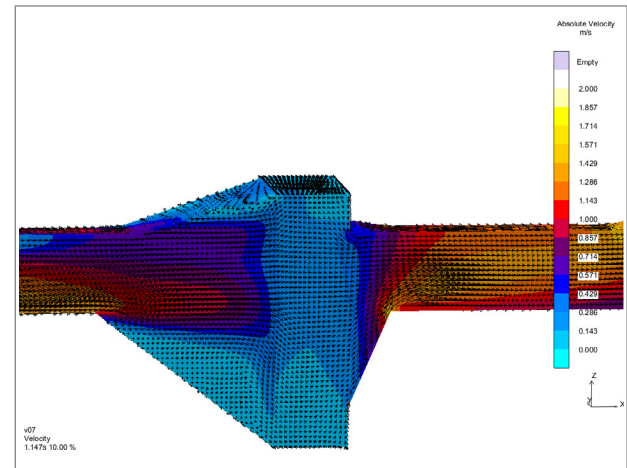


Figure 11. Flow Comparison for Vertical Filter Print with Filter Print Outlet Area Significantly Reduced at 10.0% Filled

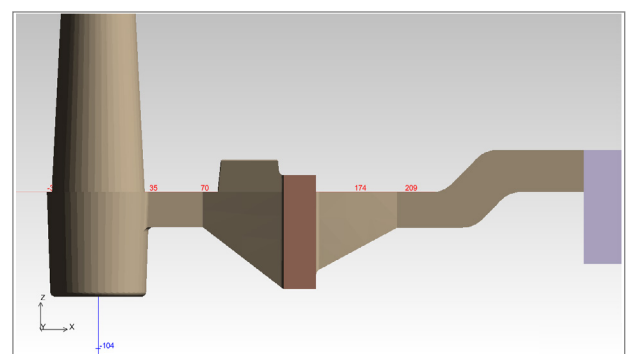


Figure 12. Standard Vertical Filter Print with Slag Trap

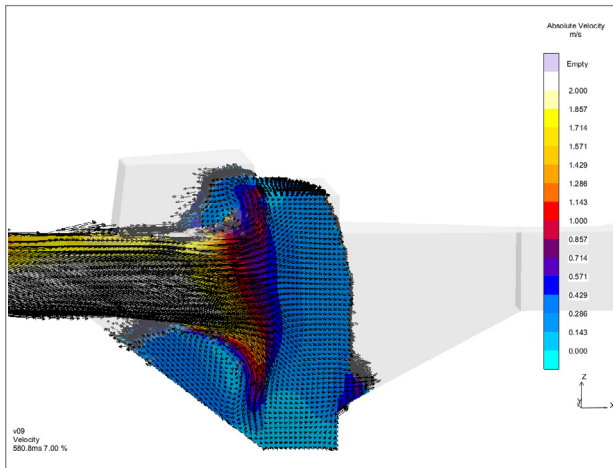


Figure 13. Flow Comparison for Standard Vertical Filter Print with and without Slag Trap at 7.0% Filled

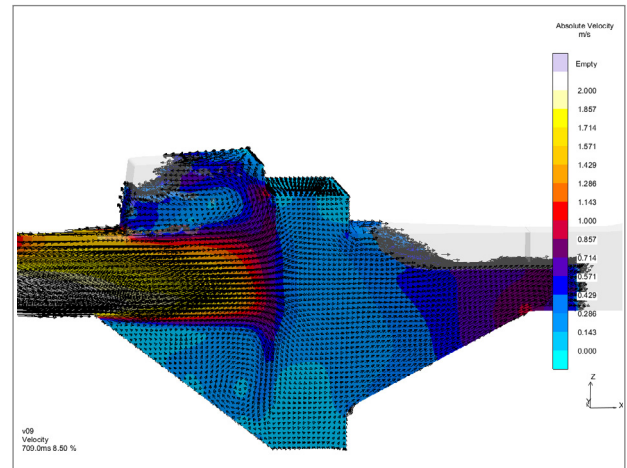


Figure 14. Flow Comparison for Standard Vertical Filter Print with and without Slag Trap at 8.5% Filled

The filter print with a properly designed slag trap displays the same the high-quality flow characteristics shown in the standard filter print with the added benefit of better filter print inlet flow and potentially better filtration efficiency. Figure 13 shows how the trap begins to work as soon as the metal reaches the filter.

Note that the bottom of the filter print inlet has filled quickly, and that the flow is washing the filter inlet face and moving upwards into the slag trap area.

At 8.5% (Figure 14), the flow is nearly stabilized, and the slag trap is forcing the initial metal into a beneficial counter-clockwise eddy current, thus potentially allowing inclusions to reverse direction and slowly float upward into the trap. The standard filter print without the slag trap also has a small area of beneficial eddy currents at the top of the filter print inlet, but very little space to trap and retain inclusions.

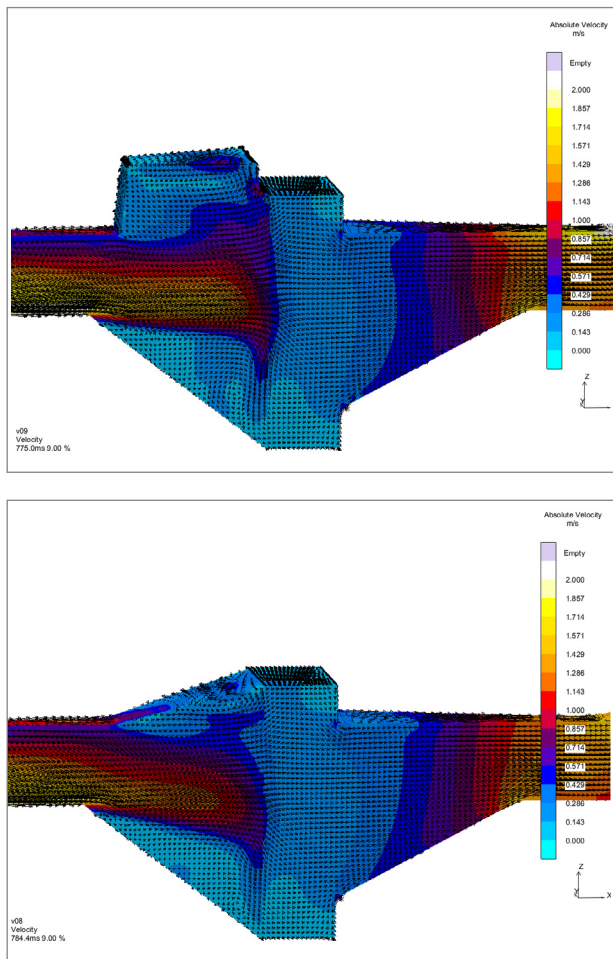


Figure 15. Flow Comparison for Standard Vertical Filter Print with and without Slag Trap at 10.0% Filled

By 10% filled (Figure 15), the filter print is fully stabilized and any inclusions that entered the slag trap will remain.

Adding a small area to trap slag in the filter print inlet improves the flow characteristics of the runner design and the ability of the filter print to trap inclusions. These are significant benefits for a minimal reduction in yield.

To summarize, the conclusions from the 2017 qualitative analyses were that the standard filter print design with a slag trap was the preferred design, followed by the standard filter print without a slag trap, if adding a trap was prohibited by pattern plate real estate issues. Sharp angles within the filter print itself were not recommended.

QUANTITATIVE ANALYSES – FILTER PRINT FLOW NUMERICAL RESULTS

Qualitative, comparative analyses, like the ones shown thus far in the paper, can provide powerful, convincing imagery of gating system changes that positively or negatively affect metal flow characteristics. Historically, comparative analyses between gating systems have provided sufficient evidence to trial and implement concepts and designs that improve metal flow and casting quality. However, an engineer is inclined to evaluate design concepts analytically, and assign absolute values with visuals. In effect, an engineer desires to combine a quantitative analysis with a qualitative analysis. That is the gist of the remainder of this paper which presents new, novel approaches and results.

Previously, only 10ppi SEDEX* filters were evaluated for the five filter print designs. For the quantitative analysis, 10, 20 and 30ppi filters will be evaluated for these five designs such that the DOE now consists of 15 separate configurations.

A good quality filter print should utilize as much of the filter area as possible and distribute the flow velocity as evenly across the filter face as possible. This allows the filter to control the flow and maximize capacity.

A novel approach to evaluate filter face flow rate was taken using the ingate options within the software. Normally, ingate material is assigned to the geometry component that connects the runner bar to the casting. In turn, the software allows for metal flow rate to be recorded for all materials identified as ingate material for the entire filling cycle.

Figure 16 shows how 25 separate ingates were modeled, just in front of the filter, such that flow rate could be evaluated for 25 discrete sections of the filter face itself.

Each numbered ingate produces a corresponding flow rate curve and allows for quantitative assessment of the variation of flow across the entrance side of the filter face.



Figure 16. Ingate Array Attached to Filter Face (image courtesy of Matt Jacobs and Konstantin Nikolov, MAGMA Foundry Technologies, Inc.)

Figure 17 shows the flow rates (kg/s) for all 25 ingate locations on the filter face for the standard filter print design with a 10ppi filter.

Most of the flow is entering the filter at six central ingate locations, namely 8, 9, 13, 14, 18 and 19.

A review of this same filter print design with 20 and 30ppi filters shows a similar pattern, with an exception. There is a slight reduction in flow velocity at ingates 13 and 14 with increasing porosity for all filter print designs.

Figure 18 shows the flow rates (kg/s) for all 25 ingate locations on the filter face for the filter print design with reduced entrance/exit areas and with a 10ppi filter.

The flow rate at location 14 is much higher (0.94 kg/s or 2.1 lb/s) than for the standard filter print design (0.75 kg/s or 1.65 lb/s). During filling, approximately 25% more metal flows through location 14 for this filter print design as compared to the standard filter print design (23 kg vs 18 kg, or 50 lb vs 40 lb). Most of the flow for this filter print is moving through locations 9, 13, 14 and 19, which constitutes usage of a relatively small section of the filter face.

A review of this same filter print design with 20 and 30ppi filters shows a similar pattern with similar exceptions listed previously.

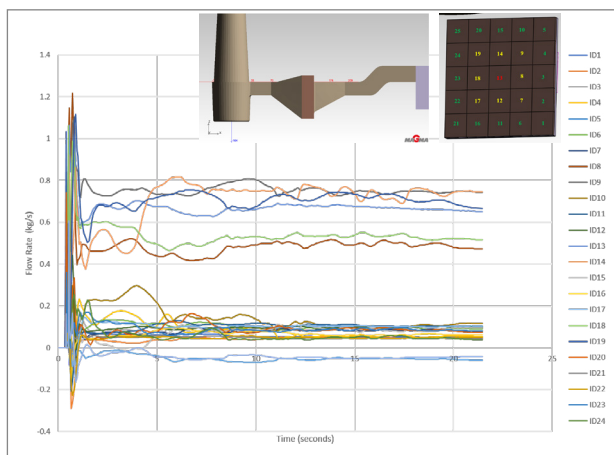


Figure 17. Standard Filter Print Flow Rates Across Inlet Face

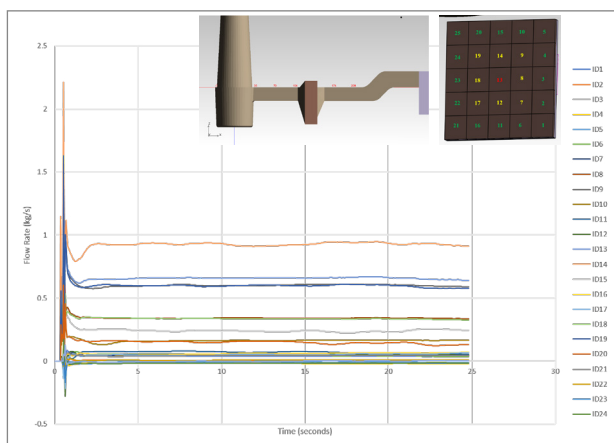


Figure 18. Reduced Area Filter Print Flow Rates Across Inlet Face

Another novel idea was implemented to quantitatively assess the angularity of the flow within the filter print. In Figure 19, two "reference" flow vectors were established, one before the filter, one after.

The flow reference direction criterion allows for the setting of a reference direction to compare to calculated flow results, and most importantly, to determine angle deviation from flow in the x-direction.

During filling, the flow vector deviance from 0 degrees along the x-axis is calculated for each mesh element at each time step during the entire filling process. Average and maximum deviation angle are calculated and used for quantitative comparison of the different designs.

Figure 20 gives a graphic example of the angle deviation calculation.

High angle deviation is directly related to higher turbulence in the filter print. An angle deviation of 90 degrees is flow that is perpendicular to the reference flow. A value of 180 degrees is backflow, or fluid flow completely opposite the flow reference direction. Low angle deviation can be considered laminar, quiescent flow.

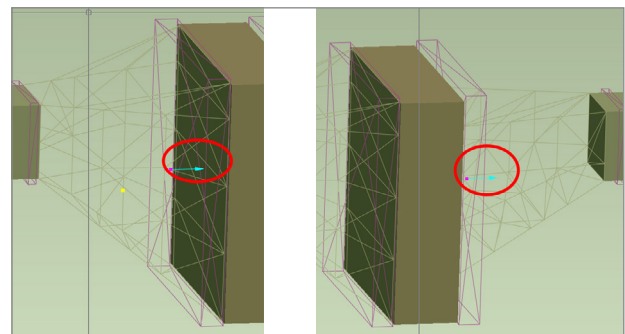


Figure 19. Flow Reference Direction Criterion (image courtesy Matt Jacobs, MAGMA Foundry Technologies, Inc.)

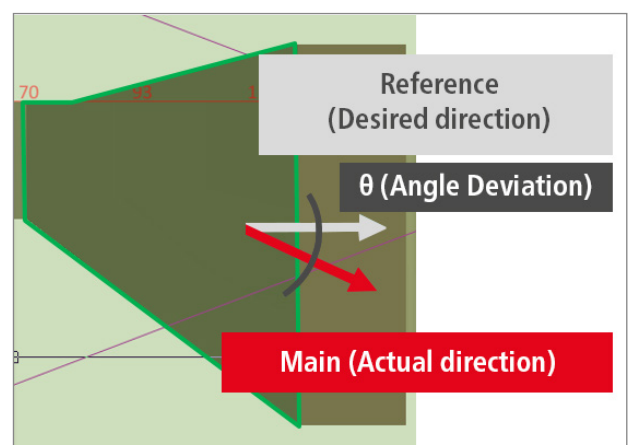


Figure 20. Flow Reference Direction Calculation (courtesy Konstantin Nikolov, MAGMA Foundry Technologies, Inc.)

The most powerful part of the evaluation is conducted using the “parallel coordinates” tool, which allows the engineer to review the effects of a filter print design on the multiple criteria at the same time. Figure 21 shows the comparison prior to analysis.

The designs are shown on the far right. Each calculated criterion is given a unique y-axis, and the values are shown with the criterion labeled at the top of the graph. The colored lines are used to connect the criterion scores for each design, and each design has a uniquely colored line. Lower scores are desired over higher scores for each criterion in this analysis.

From left to right, the objectives are:

- Average angle deviation after the filter
- Average angle deviation before the filter
- Maximum angle deviation after the filter
- Smooth filling (described later)

(Note: The maximum angle of deviation before the filter objective results are not useful because they include the effect of eddy currents at the top of the filter print and into the slag trap. Therefore, these results are not included in this analysis.)

In all cases, the desire is to minimize the values of these objectives.

The first action is to pull down the “Design” red arrow to show results for only filter print designs 1 through 5, which represents the 10ppi filter results (Figure 22).

Angle deviation after the filter is more important than angle deviation before the filter because: a) the filter will ultimately force the flow towards the x-axis and b) some flow angularity is desired before the filter to help wash inclusions off the face of the filter to float and stick on the sand at the top of the runner bar, or into the slag trap, if one exists.

After the filter, it is imperative to minimize the angularity to reduce the possibility for turbulent flow.

(In general, angularity before and after the filter, while necessary to go from the small cross-section runner bar to the filter print or from the filter print exit to the runner bar, should be minimized.)

The largest discrepancies seen in this analysis occur after the filter with respect to the maximum angle deviation. Designs 3 and 5 (with the reduced filter print exit area) have maximum angle deviation values of approximately 174-176 degrees, meaning that some part of the flow after the filter is moving upstream, or in the negative x-direction. This is obviously not ideal, as was shown qualitatively and discussed in detail in the 2017 paper.

These two designs are eliminated (Figure 23) by moving the “MAX Dev POSTFILTER” red arrow down below 174 degrees.

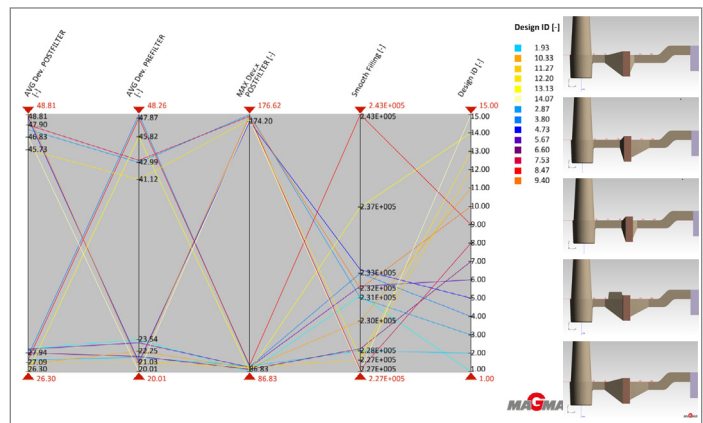


Figure 21. Parallel Coordinates Quantitative Results

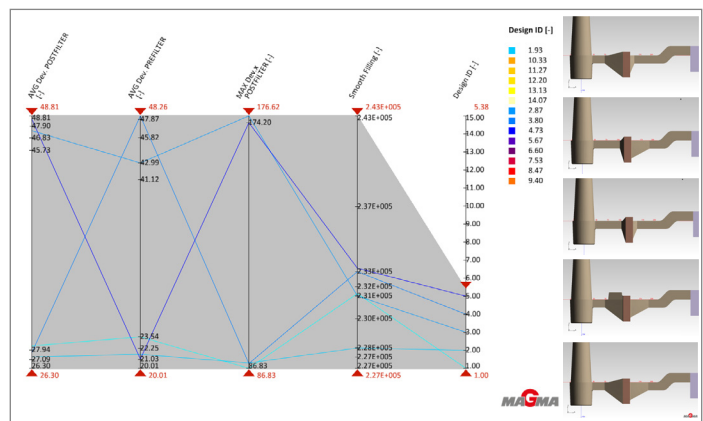


Figure 22. Parallel Coordinates Quantitative Results for 10ppi Filters

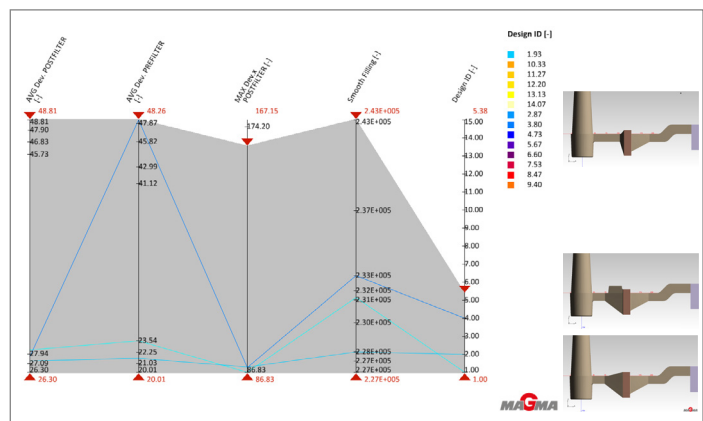


Figure 23. Parallel Coordinates Quantitative Results for 10ppi Filters – Elimination Round 1

All the other filter print designs have a maximum angle deviation after the filter of no more than 86 degrees.

The “smooth filling” criterion is defined as the maximum free surface of the cast alloy. It is a measure of metal front interaction with air, and thus the potential for inclusions.

By moving the “smooth filling” red arrow down below 2.33×10^5 (Figure 24), Design 4 is eliminated.

Surveying the two remaining designs, Design 2 (with the slag trap) has slightly better (lower) objective values than Design 1.

Further lowering the “smooth filling” objective red arrow below 2.31×10^5 eliminates Design 1 leaving Design 2 as the clear winner of the quantitative analysis (Figure 25).

The conclusion that Designs 1 and 2 are superior, with Design 2 being the best is consistent between the qualitative and quantitative analyses.

Does filter porosity alter these conclusions? No. This identical design elimination procedure, as shown in Figures 23-25 would yield the same conclusions for the 20ppi filter configurations (Designs 6-10) and the 30ppi filter configurations (Designs 11-15). As a result, this part of the analysis is not explicitly shown here but can be inferred from the next analysis.

One final analysis shows the effect of different ppi filters on the objectives calculated absolute values (Figure 26).

Each design has three of the same color curves representing the 10, 20 and 30ppi filter results. Moving the “MAX Dev POSTFILTER” red arrow down to 171 degrees shows all the results for filter print Designs 1, 2 and 4 (Figure 27).

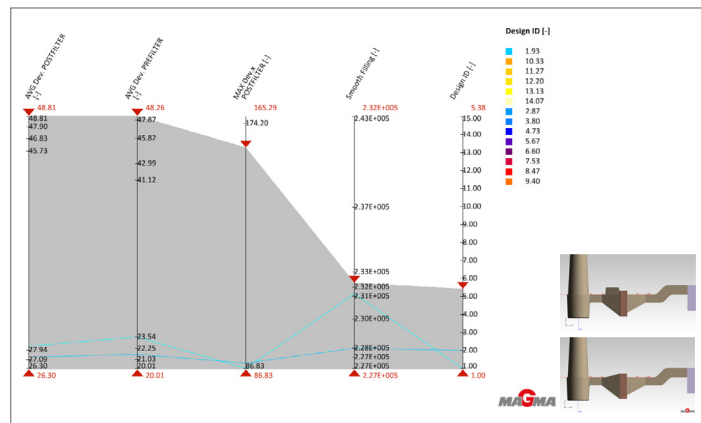


Figure 24. Parallel Coordinates Quantitative Results for 10ppi Filters – Elimination Round 2

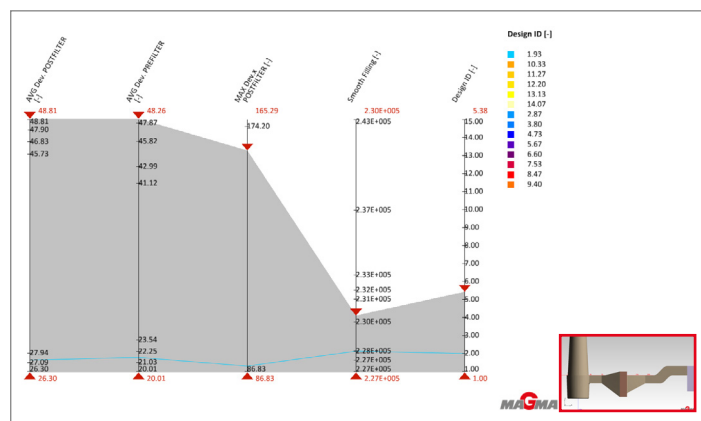


Figure 25. Parallel Coordinates Quantitative Results for 10ppi Filters – Elimination Round 3

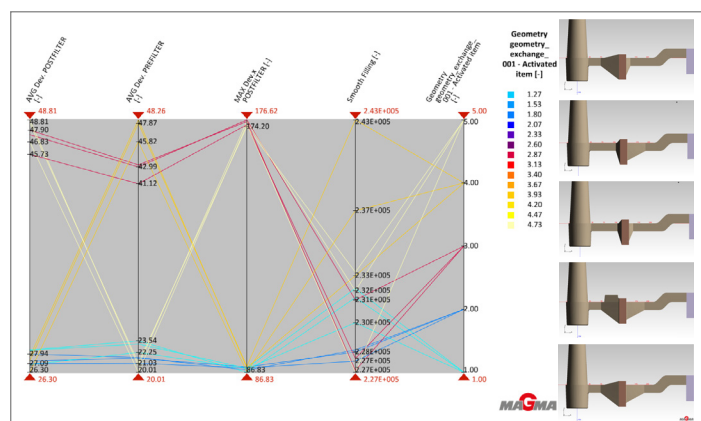


Figure 26. Parallel Coordinates Quantitative Results for All Filters

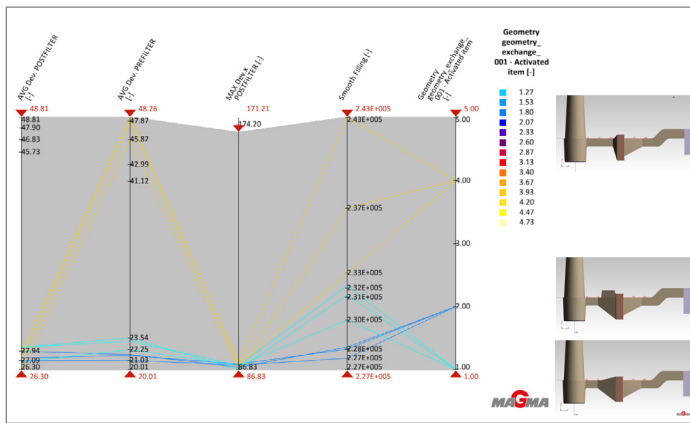


Figure 27. Parallel Coordinates Quantitative Results for All Filters – Designs 1, 2 and 4

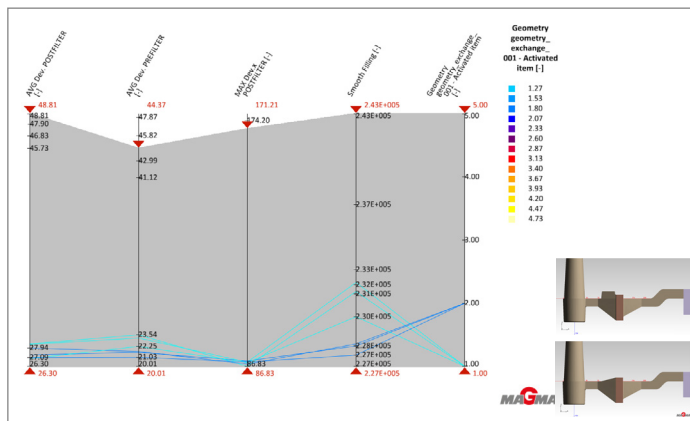


Figure 28. Parallel Coordinates Quantitative Results for All Filters – Designs 1 and 2

Moving the “AVG Dev PREFILTER” red arrow down to 44 degrees (Figure 28) shows all the results for the two best filter print designs (1 and 2).

Figures 26, 27 and 28 reveal several important points.

First, the results shown earlier are confirmed, namely that filter porosity does not alter the conclusions that Designs 1 and 2 are optimal for this analysis.

Second, there is some variability in the calculated objective results related to filter type for non-optimal designs such as Designs 3, 4 and 5, thus implying that there is some variability in performance for these designs dependent upon foam filter restrictiveness.

Third, Figure 28 shows that the foam filter restrictiveness has very little influence on the calculation of quantitative objectives for this study for the best filter print designs (1 and 2). Therefore, the best filter print designs from this analysis are independent of the restrictiveness of the foam filtration device employed.

CONCLUSIONS

Alterations are sometimes made to standard filter prints to improve yield without careful analysis of the effect on the fluid flow properties on the gating system. Quantitative analyses and the previously documented qualitative analyses evaluated the effect of several filter print design changes on the quality of metal flow in the filter print, the runner system and through the filter itself.

In general, the conclusions are as follows:

- Quantitative and qualitative analyses align to conclude
 - o Filter print Design 2 is recommended
 - Includes slag trap
 - o Filter print Design 1 is second best if pattern real estate prohibits the inclusion of a slag trap
 - o Both designs maximize the use of the front face of the filter with respect to flow rate
 - o Both designs maximize filter capacity
 - o Both designs reduce flow angularity (turbulence) before and after the filter, thus maximizing flow uniformity
- Best practice filter print design is independent of reticulated foam filter restrictiveness
 - o Caveat: filter geometry was represented using a pressure drop boundary condition
- Large reductions in filter print inlet and outlet areas, and sharp angles within the print itself adversely alter the flow characteristics resulting in non-uniform flow and turbulence
 - o Yield improvement is minimal
 - o Not recommended

Future work is planned to review additional design concepts and to validate these configurations with molten metal.

ACKNOWLEDGMENTS

The author wishes to thank Matt Jacobs and Konstantin Nikolov at MAGMA Foundry Technologies, Inc. for their ideas, their assistance with creating models and objectives, conducting lengthy simulations and their contributions to the analyses.

This paper was originally published by AFS. AFS Paper Number 20-053, published April 2020.

REFERENCES

1. Dickinson, B., Adams, A., Midea, T., "Evaluating Iron Filter Prints – 30 Years Later", AFS Transactions, 17-027, (2017).
2. Giebing, S., Baier, A. "SEDEX – Process Reliability Through Effective Quality Control," Foundry Practice, vol. 254, pp. 4 (June 2011).
3. Morales, R.D., Adams, A., Dickinson, B. "Enhancing Filtration Knowledge to Improve Foundry Performance", Foundry Practice, Special Edition, pp. 21 (May 2008).
4. Baier, A. "The Influence of Filter Type and Gating System Design on the Machinability of Vertically Parted Grey Iron Castings", Foundry Practice, Special Edition, pp. 29 (May 2008).
5. Taylor, K.C., Baier, A. "Application of SEDEX Ceramic Foam Filters on Vertically Parted Moulds Such as Disamatics", Foundry Practice, vol. 238, pp. 10 (March 2003).
6. Brown, J.R. "Foseco Ferrous Foundryman's Handbook", pp. 250-266, Butterworth-Heinemann, Woburn, MA, 2000.
7. Park, W.H. "SEDEX Ceramic Foam Filter Applications in Korea", Foundry Practice, vol. 221, pp. 2 (March 1991).
8. Matsuo, H. "SEDEX Ceramic Foam Filter Applications on Regular Production Casting in Japan, Foundry Practice, vol. 220, pp. 4 (September 1990).
9. Kallisch, W. "SEDEX – A Filter with Authority", Foundry Practice, vol. 217, pp. 18 (April 1989).
10. Rietzsch, R. Sipl. – Ing. "The Filtration of Molten Iron", Foundry Practice, vol. 212, pp. 5 (March 1986).
11. Heine, R.W., Loper, C.R., Rosenthal, P.C. "Principles of Metal Castings", pp. 223, McGraw-Hill Book Company, New York, 1967.
12. Midea, A.C. "Pressure Drop Characteristics of Iron Filters", AFS Transactions, 01-042, (2001).

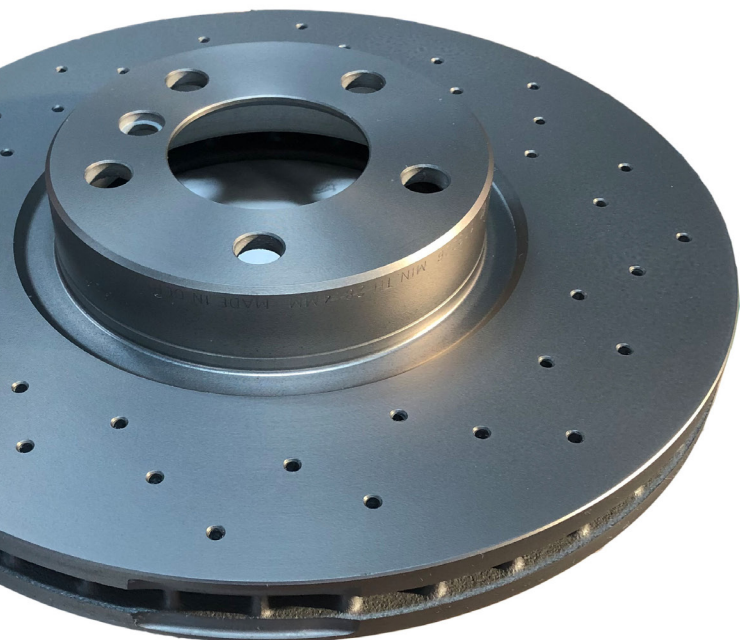
CONTACT



TONY MIDEA

REGIONAL SIMULATION
MANAGER - AMERICAS, JAPAN
AND SOUTH KOREA

Tony.Midea@vesuvius.com
+1 440 863 2762



REDUCING FORMALDEHYDE EMISSIONS FROM WATER-BASED COATINGS



Authors: Christoph Genzler and Rene Roeleveld, Foseco

Whether in our personal lives or in business, environmental sustainability is an increasingly high priority. We all must do our utmost to comply with new, more stringent and/or revised regulations in order to leave a healthier plant for the next generation.

Now is therefore the right time to apply products that can reduce the environmental impact of foundry operations.

This article will discuss water-based foundry coatings that are designed to reduce formaldehyde (FH) emissions. In doing so, they support foundries in achieving compliance with the latest EU regulations of FH release emissions in coating drying processes.

INTRODUCTION

All water-based systems are susceptible to the growth of microorganisms, such as bacteria and fungi, which can influence the performance of those systems and lead to significant changes during application. Microorganisms can also impact the health of the operators who use contaminated products.

In order to avoid such effects and protect water-based systems, biocides are included in their composition. In the foundry environment, water-based coatings are the main products that require this type of protection.

The biocides commonly contain FH, which is a powerful antibacterial and antifungal agent. This FH is released under specific conditions, such as those found in coating drying processes, and therefore contributes to the overall FH emissions of the foundry.

This presents a challenge, however, as FH is considered a harmful substance and regulated as such by the EU. The EU regulation on the emission of harmful substances (2008/50/EG) has recently been revised to further reduce allowable FH emission levels from 20mg/m³ to just 5mg/m³.

Even foundries with exhaust gas treatment facilities are required to adopt the new limits.

As an example, the revised directive has been translated for Germany as the new TA-Luft regulation, which requires re-adjustments of emissions levels at old and/or existing plants. In many cases, this would lead to investment in new gas treatment systems. The new limits have been in force since Feb. 2020.

Foseco has taken the challenge on board with a new water-based coating that helps foundries reduce their FH release emissions at the point in the process where concentration is highest: the exhaust chimney of the core drying plant.

This article will not discuss FH levels in Foseco coatings as such, however, but the total FH emissions to which the coating drying process contributes.

A COATING FOR REDUCED FH EMISSIONS

Foundries applying water-based coatings are following an established trend away from solvent-based coatings in order to better comply with environmental demands. However, these water-based products require protection against microbiological attack:

Water based coating – BACTERIAL INFECTION – EFFECTS/ACTIONS/ SOLUTIONS

Since the conversion from solvent-based to water-based coatings is happening with increased speed in Europe, it is necessary to direct foundries' attention to the effects of microorganisms on coating performance, which are not usually well known.



Figure 1. Bacteria infected coating in dip tank



Figure 2. Coating remains unmixed in dead areas in dip tank

PERFORMANCE ALTERATIONS IN CASES OF MICROORGANISM CONTAMINATION

- Smell
- pH drop
- Increased sedimentation
- Poor flow properties
- Reduced edge coverage
- Graphite flotation
- Much stronger coating penetration, leading to core breakage
- Syneresis
- Changed wetting characteristics
- Cracks in coating surface

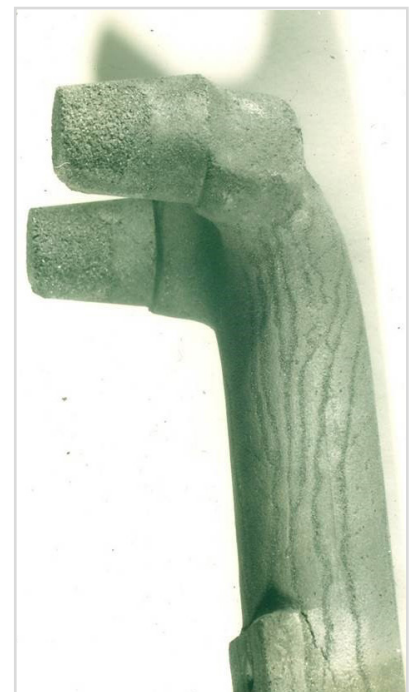


Figure 3. Syneresis when applying bacteria affected coating

PRODUCT PROTECTION

All Foseco water-based coatings have a built-in biocide that protects the product for the stated shelf life from deterioration due to microorganism growth. However, by diluting with impure water and/or introducing material into the coating that supports the growth of microorganisms over time (e.g., amine acts as fertilizer for bacteria), contamination can still occur.

These biocides remain within the applied wet coating layer and gradually release FH while the coating is dried. In cases when the drying is accelerated by use of drying ovens, FH emission levels tend to be higher in the oven and hence in the oven chimney, where the concentrated gases become of environmental interest.

COATING COMPOSITION

Compared to the rest of the components required for coating manufacturing, the biocide is only a very small proportion (< 0.1%) of the whole, but still contributes to the overall FH level.

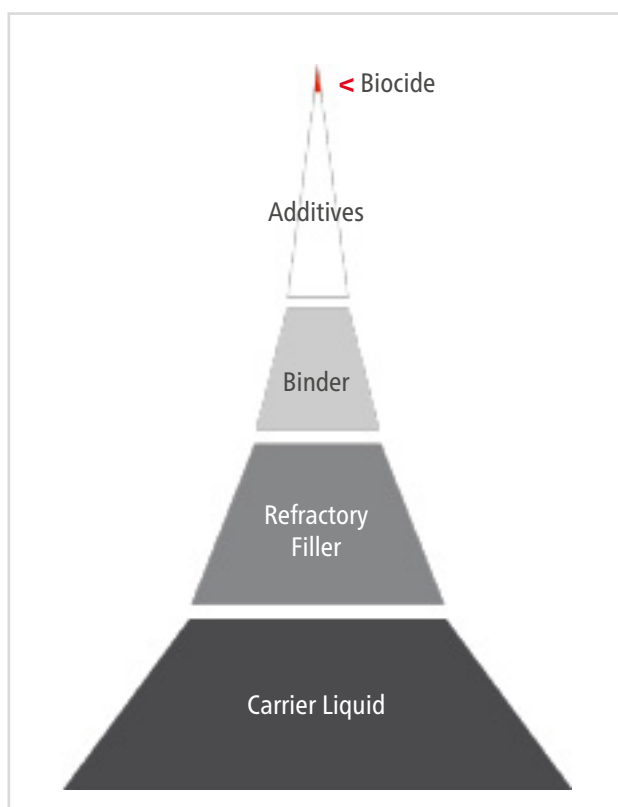


Figure 4. Coating composition

FH EMISSIONS IN FOUNDRIES

During the casting process, various FH emissions occur in a foundry, such as:

- In the melt shop during pouring,
- During shake out, due to decomposed binder components,
- In the core shop during sand/binder mixing, core/mould making and coating drying.

FH is a gas that is unfortunately not easy to measure. This is because of its nature and reactivity with other chemicals and because it might be a reaction product released when a chemical component alters, e.g., during curing, drying, and gassing processes. All those who have assembled flat-pack furniture will know the smell of FH, however, as it is used in many wood-based materials, such as particleboard, as well as many textiles.

If we concentrate in the following discussion on the core shop environment only, admittedly a lot of different odours are noticeable. Usually, the air of a core shop is exhausted and possibly treated. It is then commonly released via the chimney to the atmosphere.

For local authorities responsible for monitoring and controlling gas emissions, the exhaust chimney is the major point of concern. Here gas samples at different times and plant loads may be taken to check gas release levels – an expensive and complex process, in which a lot of influences have to be considered.



Figure 5. FTIR test set up



Figure 6. Sample holder transfer to drying oven

For FH in particular, a common industrial standard test does not exist. Foseco therefore had to develop a reliable test method, that would also help to further develop new products.

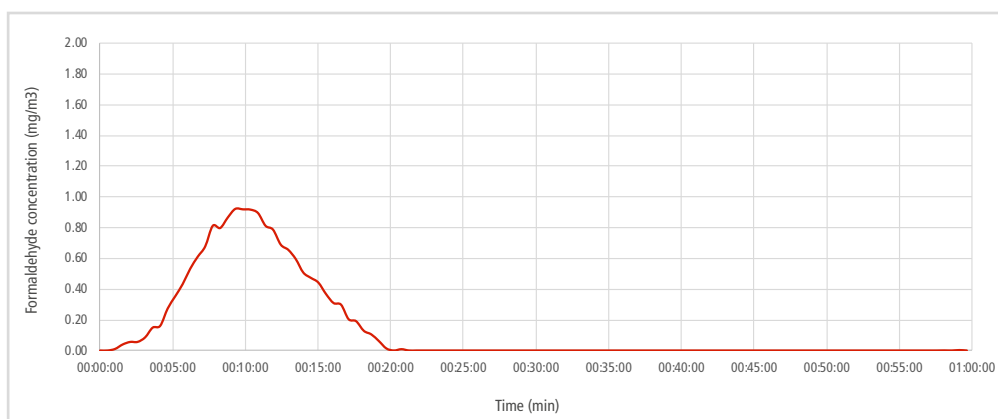
After evaluation of different ways to determine FH emissions, we found FTIR (Fourier Transform Infrared) spectroscopy most suitable, being accurate to the necessary standard and because the equipment is compact.

The test set up consists of a sealed drying oven containing a fixture to hold the sample, a heated exhaust sampler and heated pipes to avoid any condensation. The heated pipes are connected to the gas analyzer, which can then determine different pollutant gas streams, even those that occur concurrently.

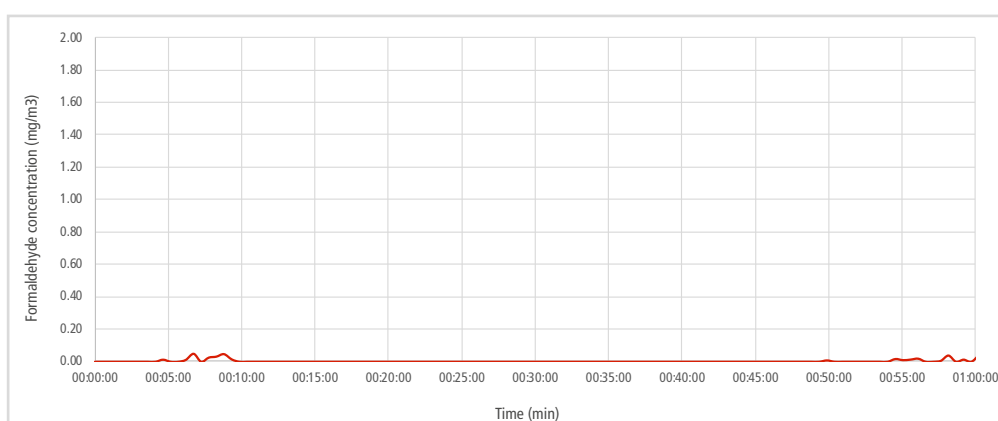
The tests are conducted over a period of 1 hour and enable Foseco to target development of new products.

To help customers to comply with new set limits, our first focus was to develop a coating that does not release FH during the drying period, but still offers the same protection against microbiological attack. During this phase quite interesting observations were made.

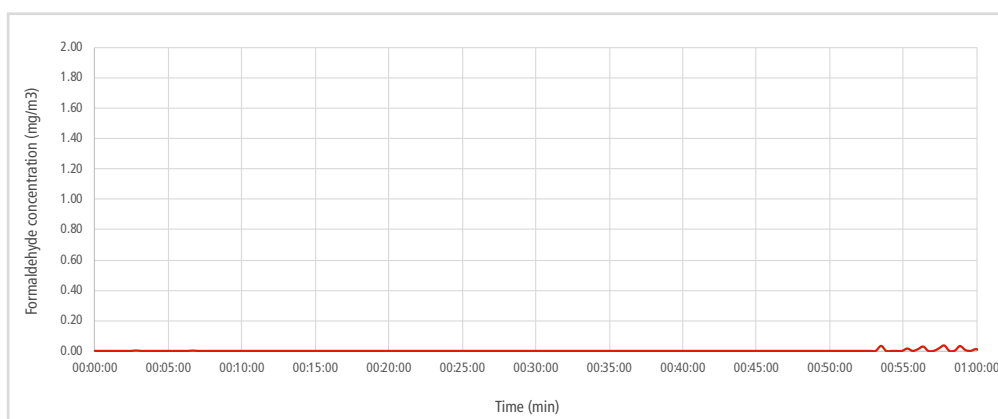
FORMALDEHYDE EMISSION PATTERN AT 150°C IN DRYING OVEN



Graph 1: Fresh ColdBox core, as-made

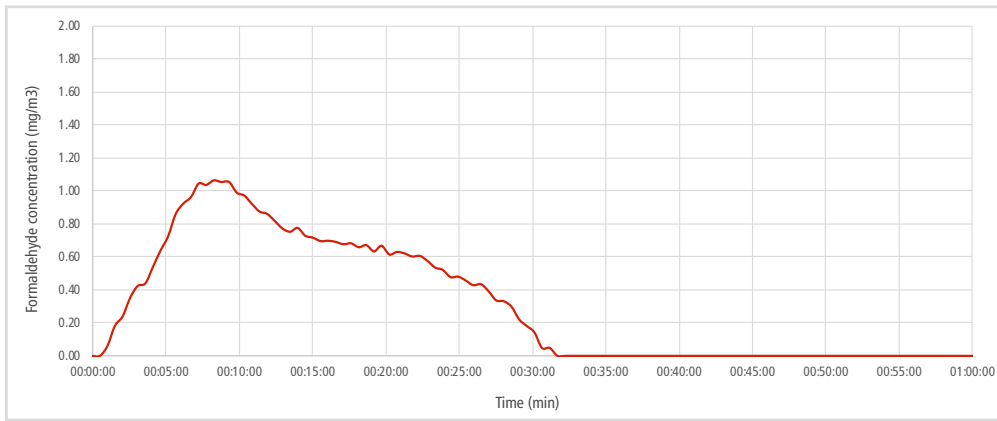


Graph 2: PUCB core aged for 3 days

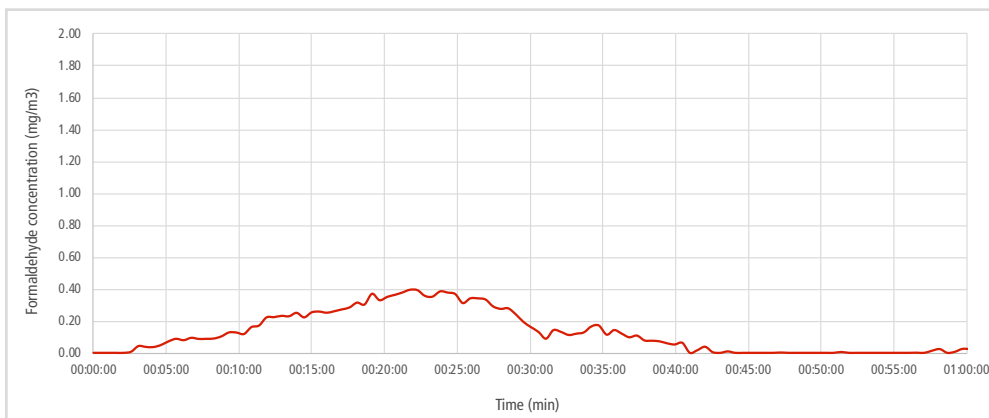


Graph 3: PUCB core aged for 11 days

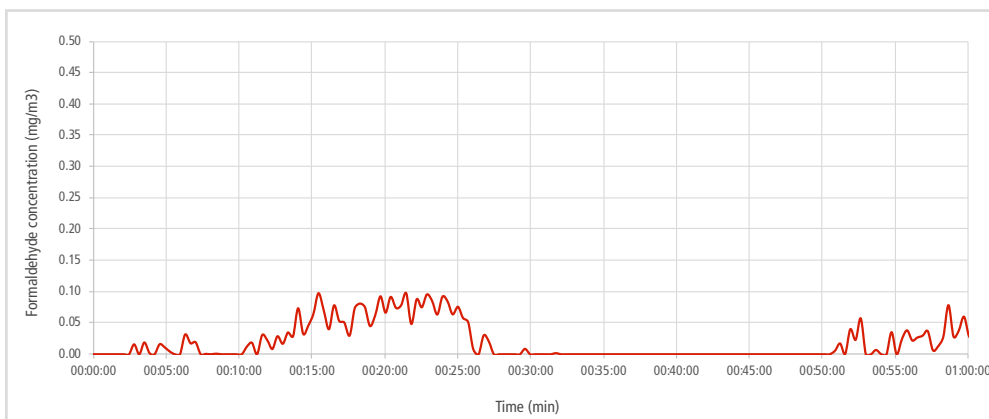
Only the freshly-made core releases a significant contribution to overall FH emissions. The binder related FH emissions observed in the drying oven are impacted significantly by the core storage duration



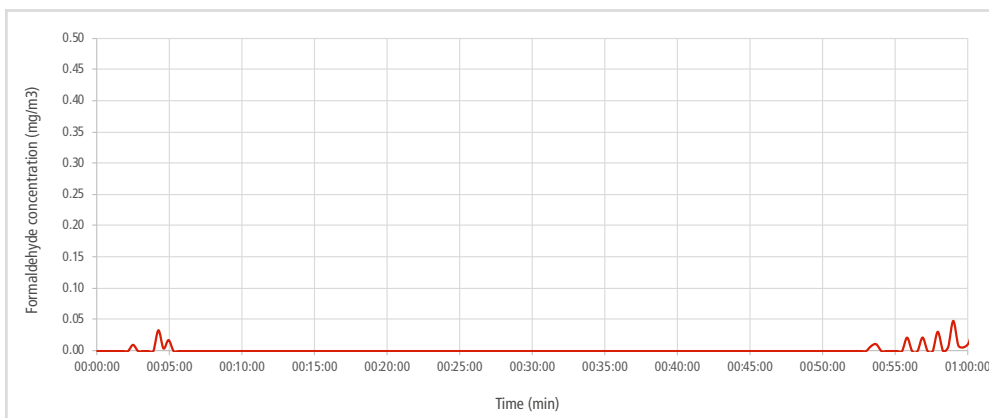
Graph 4: FH emissions from fresh, as made PUCB core with standard coating



Graph 5: FH emissions from fresh, as made core with new SEMCO* FF coating



Graph 6: FH emissions from cores aged for 11 days with standard coating



Graph 7. FH emissions from cores aged for 11 days with new SEMCO FF coating

CONCLUSION

Beside the applied coating, there are quite a number of other FH-releasing items in a core shop, such as binders and additives, that contribute to the overall FH emissions. On top of this, during several process steps, e.g., core blowing, drying and storage, FH can be released by components that reassemble / restructure / convert to different chemicals and set FH free as a step in this alteration process.

During the above FH investigation, it became obvious that the new SEMCO FF generation of coatings is only the very first step for modern water-based coatings that will help foundries to comply with the latest EU regulatory requirements.

The next step for coating development will be to evolve the coating into a FH barrier, where the FH-free coating actually absorbs FH released from the sand binder or additives.

All this is combined with a final opportunity to optimize the drying process by incorporating colour change on drying technology. This quickly and easily allows core shop operators to see when the drying process is complete, optimising energy consumption and hence reducing costs and the carbon footprint of core shop operations.

REFERENCES

All work mentioned in this paper was undertaken in Foseco laboratories and represents the results of those investigations.

CONTACT



CHRISTOPH GENZLER

EUROPEAN
PRODUCT MANAGER
COATINGS

christoph.genzler@vesuvius.com
+31 7424 92 195

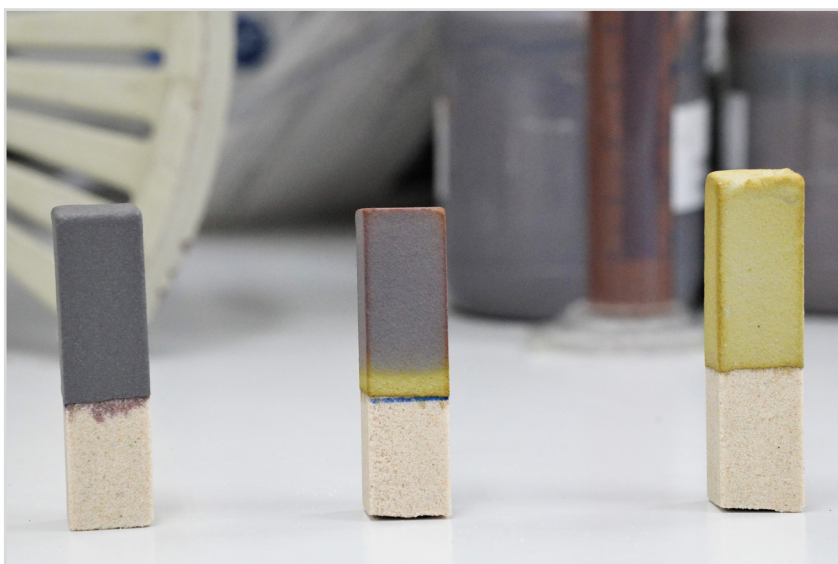
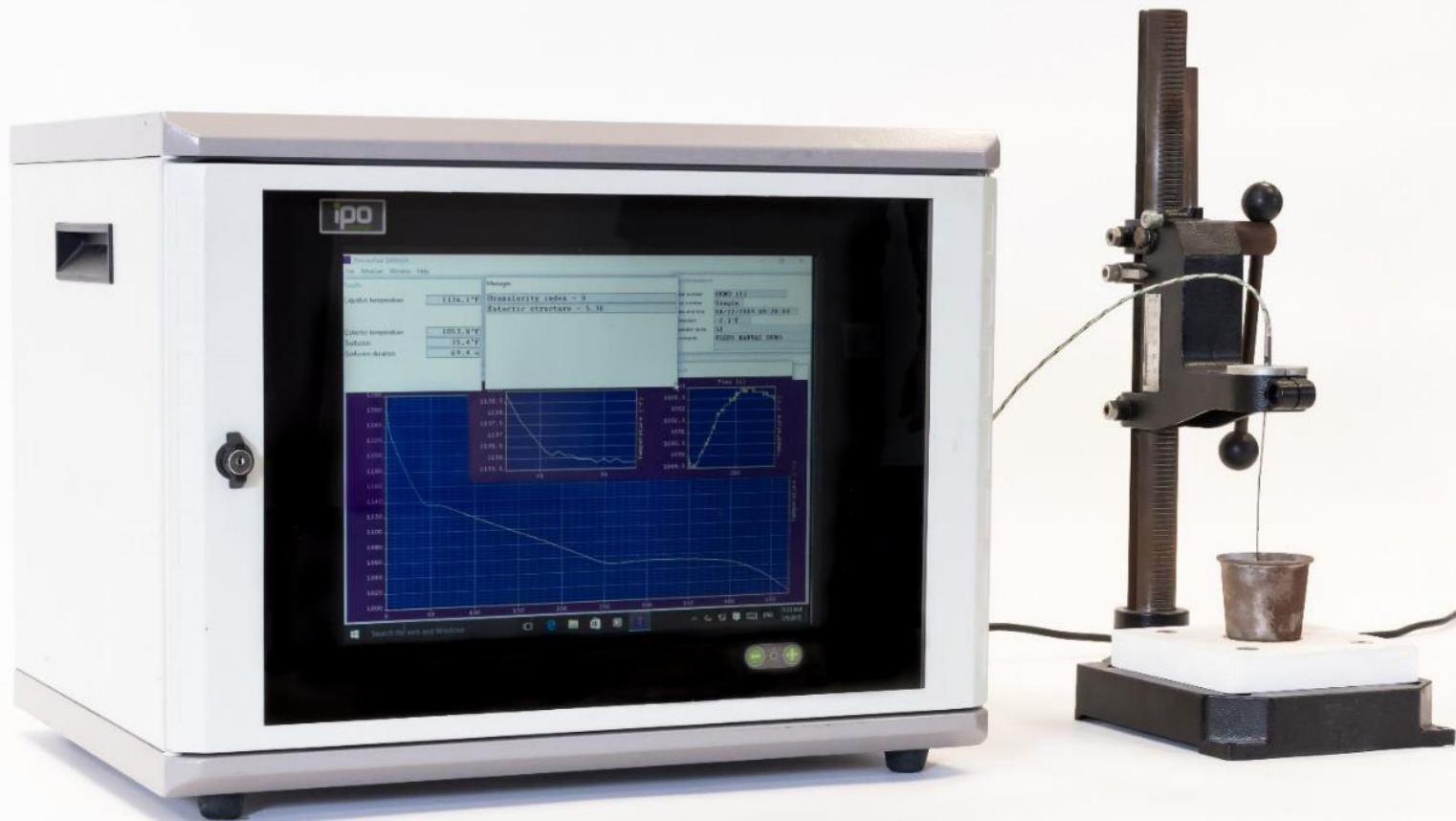


Figure 7. Coating colour change on drying

DISCOVER MORE

Want more info about reduced formaldehyde emission coating

WATCH VIDEO



AN INVESTMENT CASTING FOUNDRY EXPERIENCE IN IMPROVING DEGASSING AND GRAIN REFINING IN MOLTEN ALUMINIUM ALLOYS



Authors: Robert Zebick; Atlantic Casting & Engineering and Brian Began; Foseco Foundry Division, Vesuvius PLC

The requirements to degas, flux and grain refine molten aluminum alloys for investment casting are well established. The evolution of casting buyer requirements; now requiring larger castings or more complicated geometries than the previous generation, continually require better and more consistent melt treatments for the molten aluminum. Fortunately, several recent technological advancements have allowed degassing, flux and grain refining to be higher performing and more environmentally-friendly than were historically achievable.

This paper will report on the efforts of Atlantic Casting & Engineering (ACE) in Clifton, NJ to implement an improved aluminum alloy treatment process to keep up with the demands of industry. In addition to the process of implementation, this paper will document the rationale and evaluation process for implementing the process improvements. Finally, the paper will discuss the economic, technical and environmental benefits achieved upon complete implementation of the new treatment process.

INTRODUCTION

The subject foundry, Atlantic Casting & Engineering, is privately-owned and has been in business for over 80 years. The foundry manufactures high-precision and geometrically complex cast parts, primarily for the aerospace market, but also serves the military, electronics, transportation, medical and various other marketplaces. The operation features two different mold making processes, handling parts up to a 30" cube, and pours approximately 7000 lbs. of aluminum per day. The operation includes various paste and liquid wax injection machines, ranging from 5 to 100 tons. The investment shell area features both automated and manual dipping processes, followed by autoclave dewaxing. Seven electric melting furnaces are used to process approximately 7000 lbs. of metal per day, with up to 15 different aluminum alloys. Finally, the post-casting operation boasts a variety of equipment for finishing, heat treat, and straightening of castings, and a full CNC machine shop.

INCUMBENT MELT TREATMENT PROCEDURE

The foundry melts and pours an array of aluminum alloys including 201, A203, A205, C355, A356 and F357. These melts are melted and prepared in one of six electric-resistant crucible furnaces ranging in size from 1200 lbs. to 250 lbs. in capacity. All foundry elemental additions are made into the furnace directly rather than in the hand ladle prior to pouring.

The historical method for treating aluminum in the subject foundry entailed adding metallic-form TiBor (5%Ti, 1%B) pucks into the melt at a rate of .25% the weight of aluminum to be treated. The additions were made prior to the degassing process, which utilized an iron-cross or gear shaped rotary impellor connected to a simple pneumatic drive degassing unit that is raised, lowered and transported via an overhead hoist. High purity argon was the purge gas used during the 30-minute rotary degassing cycles.

In addition to rotary degassing, hexachloroethane degassing pills were used to provide both cleaning and additional degassing of each melt. The hexachloroethane degassing pill treatments were 10 minutes each and were added at a rate of 0.15% the weight of aluminum to be treated.

Only elemental spectroscopy of the Titanium (Ti) levels was historically used to evaluate grain refinement, with a typical target level of 0.15% (+/-0.02%) by weight. A standard reduced pressure test (RPT) was performed to assess degassing efficiency by placing a standard sample cup under a vacuum pressure of 27.5 (+/-0.5) inches of Hg for 7 minutes. A picture of the reduced pressure testing apparatus appears in Figure 1.

Once solidified, the RPT specimens were subjected to the hydrostatic displacement technique, i.e., a ratio of weight in air and a weight in water, to determine the specimen's specific gravity. The minimum threshold specific gravity for each alloy poured appears in Table 1.



Figure 1. Picture of the RPT apparatus used to assess degassing efficiency.

Alloy	Specific Gravity Specification Minimum
201	2.70
A203	2.70
A205	2.80
C355	2.65
A356	2.65
F357	2.65

Table 1. Alloys and specific gravity threshold minimums

THERMAL ANALYSIS TESTING

It has been established that grain refinement can beneficially affect feeding, fluidity and mechanical properties in aluminum castings.^{1,2} Hence, inadequate grain refinement can yield shrink voids in aluminum castings. Moreover, it is established that too much Sr can cause porosity in aluminum-silicon alloys also resulting in porosity in cast aluminum.^{3,4} Accordingly, it was decided to assess the grain refinement and eutectic modification levels to see if an improved practice was possible.

A THERMATEST 5000 NG III thermal analysis (TA) unit was used to assess the grain refinement (or grain fineness) and eutectic modification (or eutectic structure) of the treated melts after they were prepped for pouring. Thermal analysis involves collecting data of temperature versus time of a solidifying melt sample and comparing the curve to a set of known curves algorithmically. A photograph of the subject TA unit is shown in Figure 2.

The TA algorithm analyzes the sample curve liquidus and computes a score on a scale from 1-9 for evaluating grain fineness (GF). A score of 1 references a curve that compares perfectly with curves exhibiting no grain refining. In contrast, a GF score of 9 is achieved when the sample curve compares with those curves known to have produced "perfect" grain refining of melts with the same alloy composition. A pictorial representation of the subject grain refinement levels is provided in Figure 3.

The TA unit is also capable of assessing eutectic modification effectiveness as well. Like with grain refinement, the TA device compares experimentally derived temperature/time curves to known standards and computes a score on a 1-7 scale. The scale for measuring eutectic structure (ES) differs from grain refining in that a score of 7 does not denote perfect modification, but rather a condition in which too much Sr has been added and eutectic shrinkage would be expected. Typically, 356 alloy casters who are intentionally modifying the Si eutectic in their melts target a range of 4 to 5.5 on ES. ES values lower suggest insufficient modification and ES values higher suggest too much Sr modification.

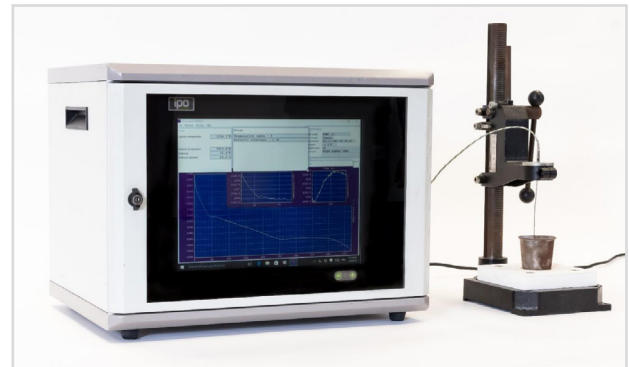


Figure 2. Photograph of the TA unit used in the melt assessment.

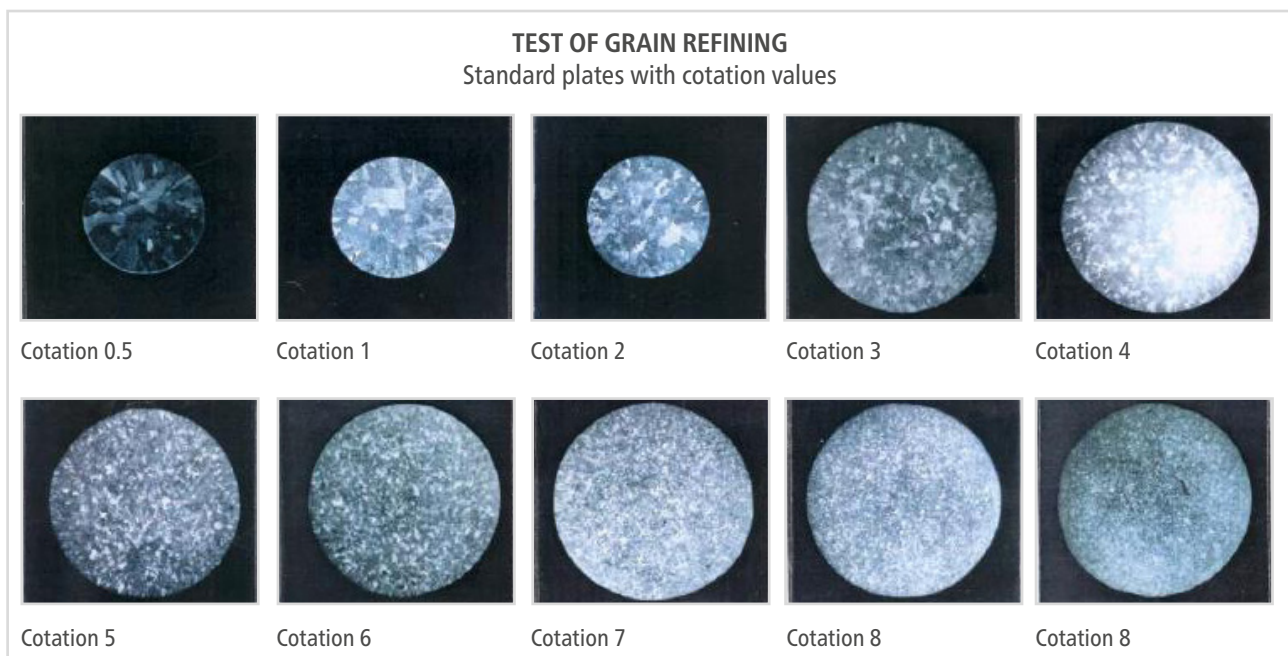


Figure 3. Pictorial representation of the grain refinement levels as measured by the TA.

The results of the TA evaluation of the incumbent process are presented in Table 2. It should be noted that no efforts are typically made to intentionally modify the eutectic silicon so a low level of near 1 was expected for the ES. Fortunately, the level of modification was so low that any effects would be negligible and what modification may have been performed should not prove problematic.

The results of the TA analysis clearly show an opportunity for improvement in grain refining as the maximum level of 9.0 was not achieved in any of the three alloy (355, 356, 357) melts benchmarked. Hence, a project to improve the grain refining was initiated.

SALT FORM GRAIN REFINING

Before there was grain refining with metallic additives such as TiBor, grain refining was predominantly achieved via salt pucks. The salt pucks would decompose and react at the holding temperatures of molten aluminum to form metallic nuclei in situ. Examples of nuclei created from salts include, but are not limited to, TiAl₃, TiB₂ and AlB₂. These examples of nuclei were chosen for the listing as they are the same nuclei formed from metallic TiBor. More information on grain refining can be found in the referenced paper authored by Began and Careil.⁵

Unfortunately, salt form grain refining with pucks fell out of favor since the pucks were buoyant in aluminum requiring that they be plunged with a stainless-steel bell jar. The elemental contamination of Fe from the stainless-steel bell jar would yield both chemistry and mechanical property problems in aluminum so an improved grain refining methodology was required. Metallic form TiBor overcame the buoyancy problems of salt form pucks so despite being costlier and largely less effective than grain refining with salt form pucks, it gained widespread adaptation since, for the moment, it resolved the issue of Fe contamination.

More recently, a novel granular salt flux form grain refiner was developed within the past decade to be an improvement over metallic form TiBor. A recent paper documented the success achieved both technically and financially in converting from metallic form TiBor to the reference salt form grain refiner at Littlestown Foundry in Littlestown, PA.⁶ The salt form grain refiner can be applied without steel tools so it overcomes the Fe contamination issues associated with the pucks. In contrast to the pucks, the granular flux form grain refiner can be integrated with a Metal Treatment Station (MTS) so that only graphite and inert ceramic components contact the aluminum during its application. The salt form grain refining flux has the additional benefit of being a very strong cleaning flux capable of reacting with oxides to chemically separate them from aluminum.

As previously indicated, the predominant way for reacting the salt form grain refining flux is via a metal treatment station (MTS). In a MTS, a vortex is temporarily created by withdrawing a vortex breaker baffle board and increasing RPM's of the graphite shaft and rotor used in the rotary impellor degassing process. PLC controlled additions of the treatment flux are added into the vortex and mixed to complete reaction prior to the vortex breaker baffle board re-engaging the melt, effectively stopping the vortex. After the vortex has been stopped, the MTS completes a standard rotary degassing process and the treated metal in the ladle or crucible is used for transferring and/or casting.

Alloy	Grain Fineness (GF)	Eutectic Structure (ES)
355	6.9	2.51
356	6.2	1.27
357	7.5	N/A

Table 2. Results of TA evaluation with incumbent procedure

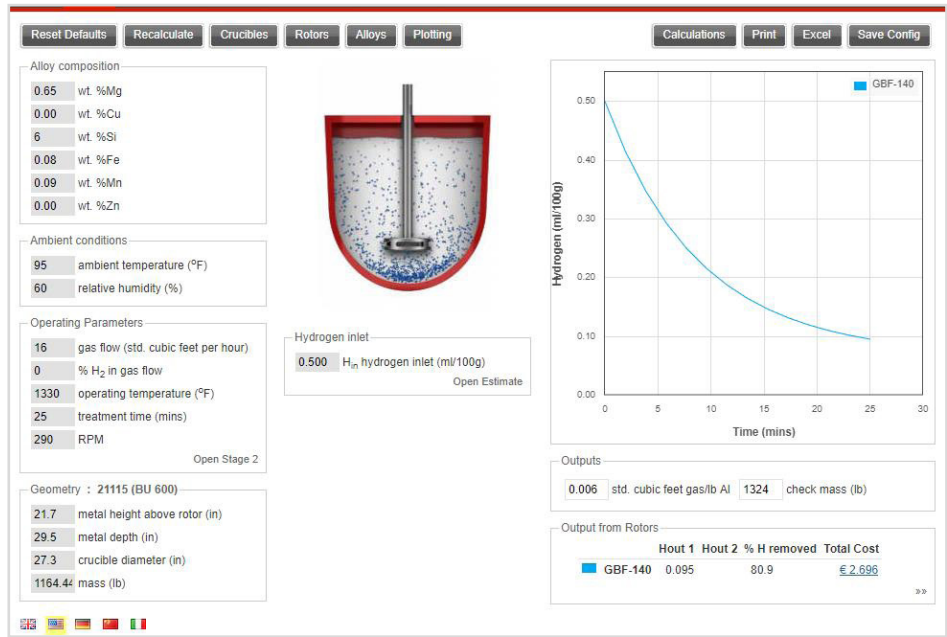
EXPERIMENTAL PROCEDURE

DEGAS MODELING

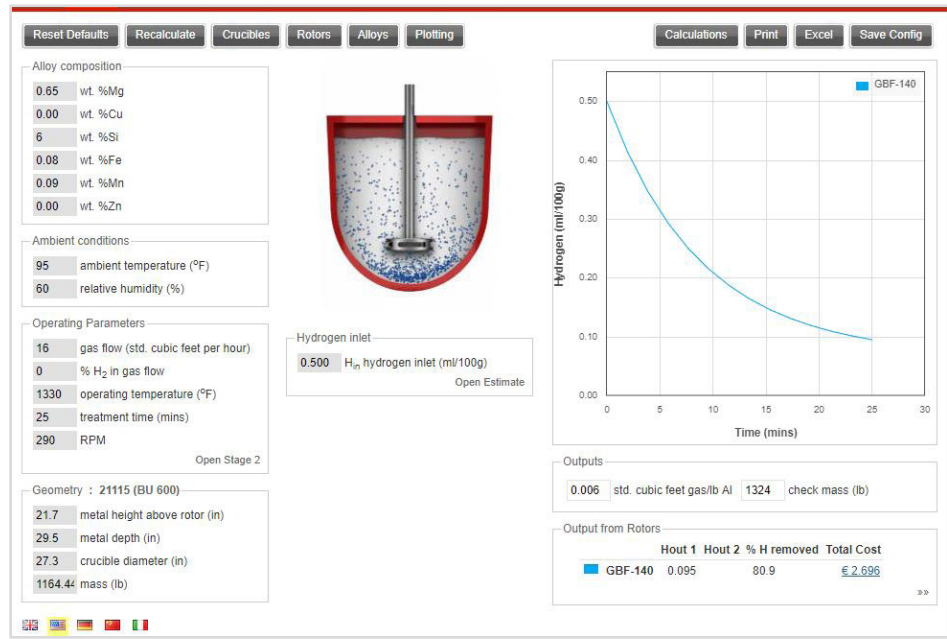
To assist with achieving optimized hydrogen removal, a degassing model was utilized to determine a minimum cycle time.⁷ The parameters were plugged in using 357 alloy since it is generally the toughest of the aforementioned alloys to degas in terms of cycle time. The chosen conditions tended towards the extremes where degassing is most difficult, e.g., high temperature and humidity. The parameters for the new procedure model are presented in Table 3. A model was prepared as a best estimation of the incumbent process as well with the only change being the rotor design being run at the traditional rpm, flow rate, etc. The results of the model for both the incumbent procedure and the newly proposed procedure are presented in Figures 4(a) & 4(b), respectively.

1200 lb Crucible	XSR 220 rotor
357 Alloy	0.50 ml H2 / 100 g Al starting level
1330° F melt temperature (*)	600 s minimum treatment time (*)
60% relative humidity (*)	95° F ambient temperature (*)

Table 3: Parameters for degas modeling



(a) Modelling of incumbent degassing procedure



(b) Modelling of proposed degassing procedure

Figure 4. Results of Degas Modelling 357 in 1200 lb. Furnace.

The results of the degas modelling confirmed that in even tough conditions, the new rotor design and unit combination should be able to degas the melt in approximately 6-8 minutes under ideal rotor and baffle plate conditions. A 13-15 minute average cycle should be more than sufficient for when rotor wear, belt wear and perhaps baffle plate wear lead to a slight reduction in degassing performance. The model approximation performed for the incumbent process suggest that 25 minutes are required to degas the same melt in similar conditions; hence, a 30 minute historic degassing time was apropos although experience has shown that when the rotor and/or baffle plate were worn, a repeat cycle was often required.

A dimensional schematic of the MTS degassing unit designed for trials appears in Figure 5.

The unit can be moved into place by either a fork truck or an overhead hoist and operates by being set upon the melt furnace targeted for treatment. The unit employs a retractable carriage that will automatically lower the degassing shaft, rotor and baffle plate into the melt during treatment and automatically withdraw the degassing shaft, rotor and baffle plate at the end of the treatment. The unit is designed to withstand the heat of the melt to be treated and to pass purge gas only during the cycle. The unit is outfitted with a hopper to hold the grain refining flux and an auger drive system to deliver precise amounts of flux each treatment.

THE NEW MELT TREATMENT PROCEDURE

After completing the modelling, the new melt treatment procedure was tested against the incumbent procedure. Specifics of the newly evaluated procedure follow:

- Treatments with a Hoist Mount MTS unit and an improved pumping rotor design
- Treatment parameters set according to the degas modeling
- Grain refining and cleaning to be performed via the automatic additions of the grain refining flux
- Argon to remain the purge gas
- Treatment cycle will be automated to 10 mins for 600 lb. crucibles and 15 mins for the 1200 lb. crucibles
- Elimination of TiBor and Hexachloroethane pills

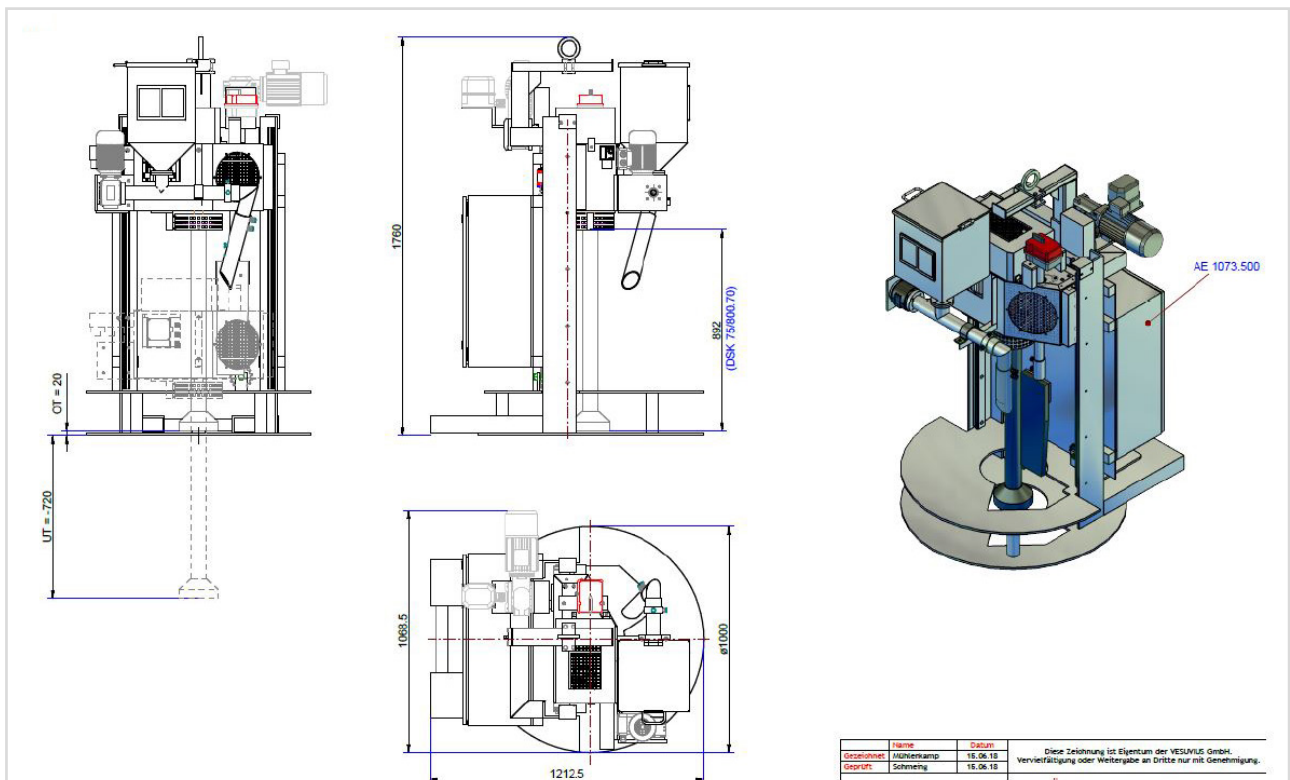


Figure 5. Dimensional Print for the Metal Treatment Station

GRAIN REFINING

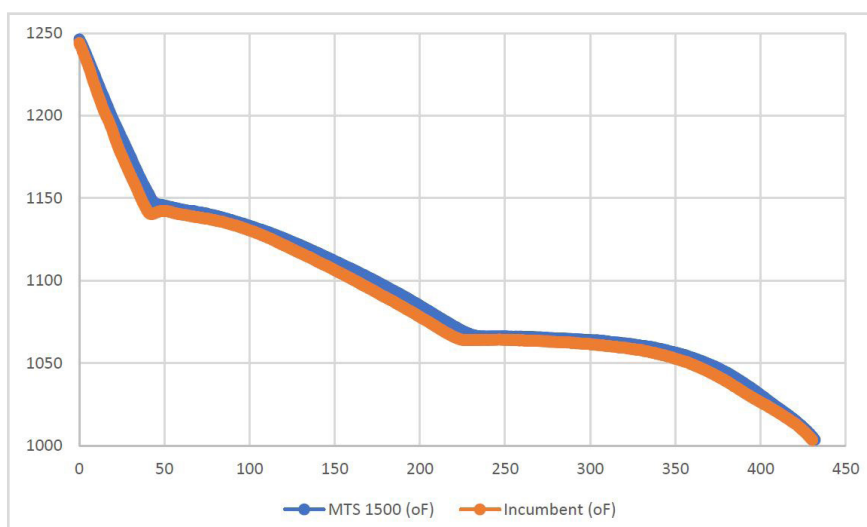
Once the MTS unit was onsite, efforts were taken to verify the effectiveness of the vortexing system with respect to grain refinement. Grain refining flux additions of 0.06% the weight of aluminum melt were added via the MTS to both 600 and 1200 lb. melts. The results of the TA testing results are tabulated in Table 4. In every treatment using the grain refining flux, a perfect GF score of 9.0 was achieved.

Alloy	Grain Fineness (GF)	Eutectic Structure (ES)
355	9.0	1.69
356	9.0	1.00
357	9.0	N/A
355	9.0	2.98
355	9.0	2.06
357	9.0	N/A

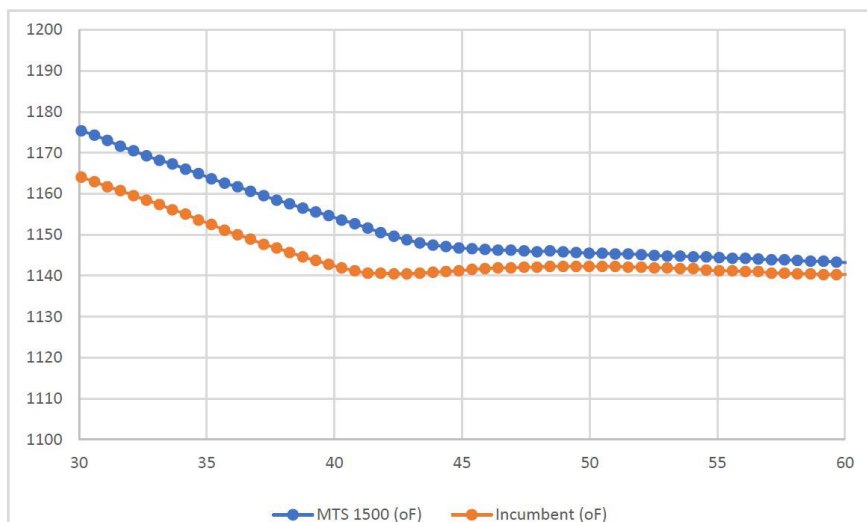
Table 4: Results of TA Evaluation with grain refining flux

TA curves taken in 356 alloys from the incumbent process (orange) and with the grain refining flux (blue) are overlayed and presented in Figure 6. Figure 6(a) shows the entire TA curve and Figure 6(b) shows a blow up view of the liquidus portion of the curve. The liquidus is the portion of the curve where the primary aluminum grain changes from liquid to solid. The TA value for the blue (grain refining flux) line was 9 while the TA value for the orange (incumbent with metallic TiBor) line was 6.2. For reference, these TA values match the readings reported in Table 2 and Table 4 respectively, for 356 alloy.

In Figure 6(b) you can clearly see some the orange line go down and then index slightly back up before indexing back down. This phenomena where the cooling curve indexes up before indexing back down is metallurgically referred to undercooling and indicates an opportunity to improve grain refining. In contrast, you do not see any undercooling in the blue (grain refining flux) line which indicates there is no opportunity for improving the grain refining in its melt.



(a) Entire TA overlay of curves for incumbent and flux grain refining



(b) Blowup view of TA curves at liquidus arrest for incumbent and flux grain refining

Figure 6. TA curves taken of both the incumbent and the flux grain refining

HYDROGEN CONTROL

Once the effectiveness of grain refining was verified, the evaluation of the hydrogen was completed. The cycle times were lowered from 30 minutes with the incumbent process to a cycle time average of 13 minutes so there was initial concern about matching performance. Fortunately, every cycle tested matched, or exceeded, the threshold specific gravity specification according to the internal RPT protocol. Moreover, a novel in situ hydrogen sensor was used to verify that hydrogen levels were equivalent or better than the incumbent procedure. For more information on the novel hydrogen sensor used to confirm performance, review the content on the work by Fray and co-workers in the referenced paper by Sigworth & Began.⁸

The results of the hydrogen concentrations taken during testing are provided in Table 5. The results are concentrations of hydrogen based on the Nernst equation and were taken from two different dates. In contrast to specific gravity where a higher number is preferred, lower values are preferred with hydrogen concentrations. The great news is that even though the new process showed a little bit better hydrogen concentration levels, even the three measurements taken from the incumbent process were strong (favorable) readings.

Alloy	Incumbent [ml/100g]	MTS 1500 April 2018 [ml/100g]	MTS 1500 October 2018 [ml/100g]
355	.10	.07 / .05 / .08	.06
356	.12	.10	N/A
357	.08	.08	.04 / .06 / .06

Table 5: Results of evaluation for hydrogen concentrations

RESULTS

The original evaluation of the new melt treatment was a success so it was implemented, monitored and verified five months later. A tabularized dataset from the adaptation appears in Table 6.

The successful adaptation of the new process brought about the following technical & productivity benefits:

- Perfect grain refinement every treatment measured with the THERMATEST 5000 NG III unit including 7 more tests run 5 months after implementation as part of the verification process
- Not a single failed specific gravity test since implementation! 25% of the treatments with the incumbent process would fail specific gravity testing allowing for 2 more melts treated and poured per day.

ENVIRONMENTAL AND SAFETY BENEFITS

There are significant environmental and safety benefits available in the elimination of Hexachloroethane degassing pills. Hexachloroethane pills decompose in aluminum aspirating gaseous chlorine ions. These chlorine ions are recognized as toxic, carcinogenic and highly reactive with many materials. Hexachloroethane pills were actively targeted to be phased out of the foundry industry in the United States starting in 1999 because of the array of detrimental side effects when the chlorine ions are aspirated. Even when Hexachloroethane pills do not aspirate chlorine ions, they are dangerous to the touch since they can adsorb to the skin causing a depression to the central nervous system according to Wikipedia.⁹

- A 69% reduction in degassing time average per day.
- 30% increase in metal poured per day.
- Effective elimination of hexachloroethane pills (without performance implications) leading to improved safety and environment.

Additionally, the following economic benefits were achieved upon adaptation of the new process:

- Elimination of the \$28.80 daily spend on Hexachloroethane pills
- Grain refiner savings of \$84.42 per day switching from metallic TiBor to the grain refining flux.
- Argon savings approximating \$4.65 per melt.

Metric	Incumbent	MTS Process	Comments
Chlorine Cost (\$/lb.)	\$3.20	0	N/A
Chlorine Usage (per/lb of Al)	0.15%	0	N/A
Chlorine \$/day	\$28.80	0	100% reduction
Ave Cycle Time (mins)	30	13	56.67% reduction
Ave Total Melts/Day	8	8	N/A
Ave Repeat Cycles	2	0	N/A
Ave Approved Melts/Dav	6	8	N/A
Success rate	75%	100%	N/A
Total Degas Time (mins per day)	338	104	69.2% reduction in degassing time
Melt (lbs./day)	6000	7800	30.00% increase metal poured per day
Tibor% Melt/lbs. per Al	25%	0	N/A
COVERAL* MTS 1582	0	0.06%	N/A
Grain Refining Cost/Day	\$104.55	\$20.13	\$84.42 or 80.7% reduction in daily spend
Argon Spend/Melt	\$11.05	\$6.40	

Table 6. Tabularized Dataset of Incumbent and New Procedure

The adaptation was reviewed for potential drawbacks and other implications it may have caused. It was hoped that the mechanical properties, particularly elongation, may go up due to the improved grain refining (as it had in the referenced paper at Littlestown Foundry); however, the mechanical properties tested before and after the new process adaptation remain unchanged statistically. Viewed from another angle, maintaining mechanical properties without using Hexachloroethane pills is a positive as mechanical properties and cleaning of aluminum melts is the predominant reason some foundries cite for not ceasing their use despite the myriad of health issues they can cause.

The baffle plate is an additional spend item (approximated at \$1500 per annum) so these new costs need to be subtracted from the total savings. Finally, the graphite components for the new system cost more per piece than the historic process components but annualized spend is expected to be less since there are shorter cycle and longer usable life of the newer consumables which are thicker and last longer. However, if (or in our case when) the operators accidentally mishandle these components a slight decrease in savings (and potentially an increase in spend) can result and during the first year an increase of graphite spend is estimated to be nearly \$1500.

Finally, the biggest difficulty with the new system is the bulkiness of the new unit, which requires a higher-grade overhead hoist and more caution from the operators because it is nearly ten times larger and heavier than the incumbent unit.

However, it is unanimously agreed that the benefits of the new system far outweigh those few difficulties that were introduced with the new unit/procedure.

An approximate payback Table appears in Table 7. After all of the cost savings in reduced argon spend, eliminating chlorine pills and lower grain refining costs are offset by the slight increases in spend on graphite and baffle plates, a payback can be calculated and was determined to be approximately 16.5 months.

Saving	Payback Calculation Component Savings
Argon	\$8,462.38
Chlorine Pills	\$7,488.00
Grain Refining	\$21,949.20
Baffle Plate	-\$1,500.00
Graphite Shafts/rotors	-\$1,459.90
Sum annualized savings	\$34,939.68
Payback (years)	1.37
Payback (months)	16.50

Table 7. Payback Calculation Table

SUMMARY

A novel method for applying a combination salt-form grain refining flux and rotary degassing system was implemented at an investment casting operation in Clinton, NJ to great success. The new treatment method resulted in an improved grain refinement practice that lowered spend, increased productivity, improved hydrogen control, delivered environmental & safety benefits and eliminated waste. The calculated payback on a new MTS unit was calculated to be about 16.5 months.

ACKNOWLEDGEMENTS

The authors would like to thank Jason Allen of Foseco for preparing the TA curve graphics and Ben Groth of Foseco for preparing the optical micrographs. Additionally, the authors would like to thank Joe Spadacinni of Weaver Materiel Services and Vernon Edwards of Atlantic Casting & Engineering for capturing much of the TA data.

Reprinted with permission by the Investment Casting Institute

REFERENCES

1. Limmaneevichitr, C., & Eidhed, W. Effect of Flux Compositions on Grain Refinement in Al-Si-Mg Alloy. TMS Light Metals Proceedings. p. 1107. San Francisco, CA: TMS (2005)
2. Dahle, A.K., Tondel, P.A., Paradies, C.J., & Arnberg, L. (1996). Effect of Grain Refinement on the Fluidity of Two Commercial Al-Si Foundry Alloys. Metallurgical and Materials Transactions A, Vol 27A. pp. 2305-2313 (August 1996)
3. Liao, H., Song, W., Wang, Q., Zhao, L., Fan, R., & Jia, F. Effect of Sr Addition on Porosity Formation in Directionally Solidified A356 Alloy. International Journal of Cast Metals. Res., 26(4). pp. 201-208. (2013)
4. Bian, X., Zhang, Z, & Liu, X., Effect of Strontium Modification on Hydrogen Content and Porosity Shape of Al-Si Alloys. Materials Science Forum. pp. 331-337, 361-366. (2000)
5. Began, B, & Careil, P. Theory and practice of grain refining for aluminum alloys – utilizing COVERAL MTS 1582. Foseco Foundry Practice Issue 268. pp 4-11 (2019)
6. Stonesifer, J. & Began, B. Degassing and Flux Grain Refining in a Continuous Treatment Well at Littlestown Foundry. 123rd Metalcasting Congress Proceedings (pp. 5-7). Atlanta, GA: American Foundry Society. (2019)
7. Simon, R., & Began, B. An Introduction to Self-Monitoring Adaptive Recalculating Treatment Technology (SMARTT) in Degassing Aluminum. Conference Proceedings. (pp. 2-7). Newport, KY: Investment Casting Institute. (2017)
8. Sigworth, G., & Began, B. Control and Measurement of Hydrogen in Aluminum. AFS 116th Metalcasting Congress Proceedings (pp. 8-9). Columbus, OH: American Foundry Society. (2012)
9. <https://en.wikipedia.org/wiki/Hexachloroethane>

CONTACT



JACOB JOHNSON

APPLICATION ENGINEERING
MANAGER

jacob.johnson@vesuvius.com
+1 440-863-2744

MELT QUALITY INVESTIGATION FOR HIGH INTEGRITY ALUMINIUM CASTINGS

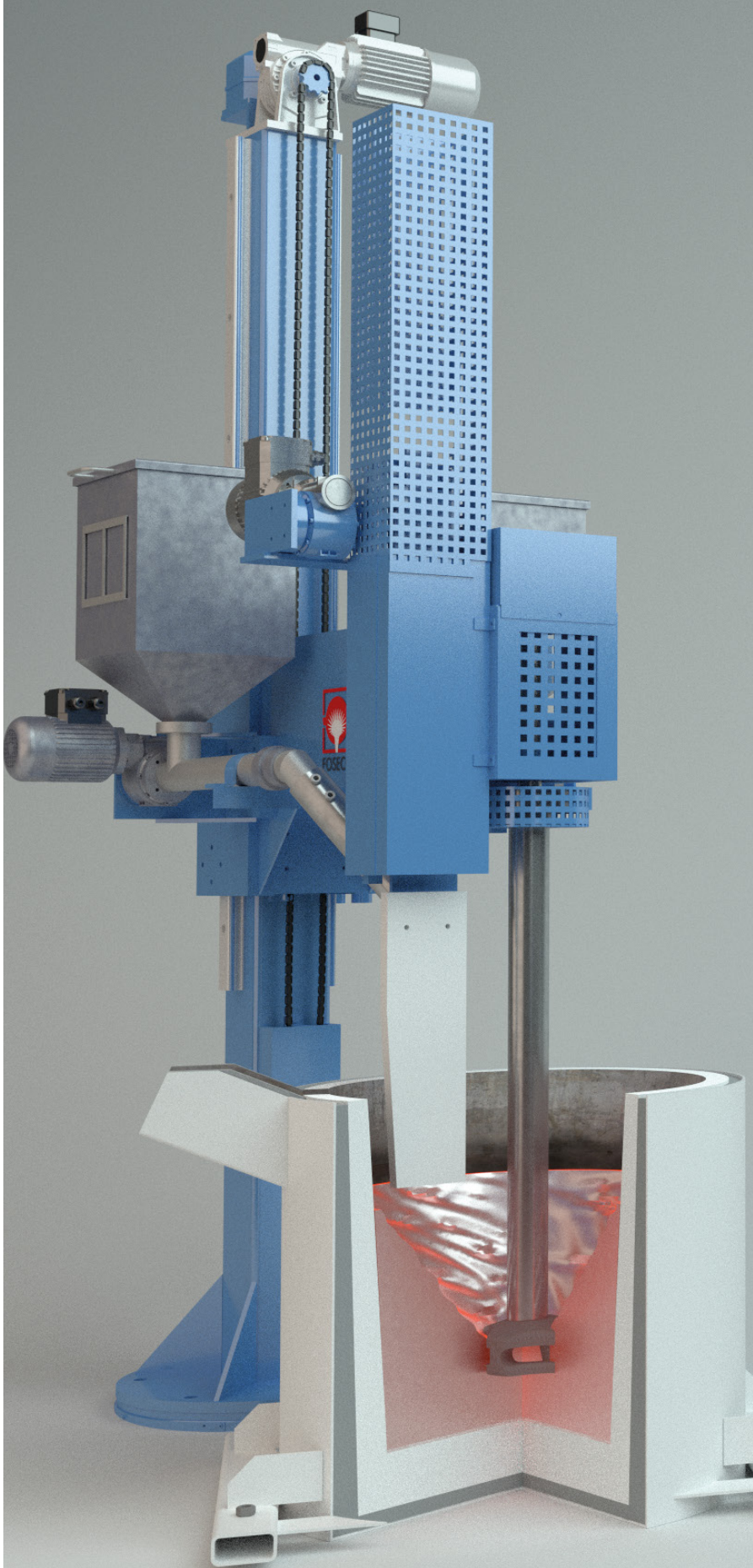
**Authors: Philippe Kientzler (MSc) and
Takehiko Okamoto, Foseco Japan,
Tenco Xue, Foseco China and Pramuk
Uhapattanapanich, Foseco Thailand**

Critical metal treatment practice and quality
analysis for aluminium foundries

This paper will review some of the latest
benefits observed with the MTS 1500
process in terms of improving melt
cleanliness when making Aluminium
pistons, low-pressure wheels or melting
Aluminium chips.

Some MTS case studies will focus on HPDC
which is becoming the largest aluminium
process driven by e-mobility.

The use of VMET (Melt Quality Assessment)
has enabled us to quantify the level of melt
quality improvement that is generated by
the MTS 1500 Process.



INTRODUCTION

Metal treatment is a critical part of the foundry process, which often has a significant impact on casting quality^{[1][2]}, reject rates and costs.

Hydrogen gas porosity is one of the primary concerns in Aluminium foundries^[3].

But oxide removal also referred to as “melt cleaning” is becoming an increasingly important step which significantly impacts the casting’s mechanical properties.

Existing cleaning practice often consists of hand fluxing or rotary degassing flux injection, but both have important restrictions or limitations.

Hand fluxing can be unreliable since it is operator dependant. Variations in addition rates, treatment times can cause major differences in efficiency and melt quality when cleaning, grain refining or doing sodium modification. This is especially true in High Pressure Die casting (HPDC) where the number of ladles or furnaces treated can exceed 100 per day.

Rotary degassing flux injection has improved some of these issues by reducing the variability due to the human factor. Unfortunately, the injection of flux through a rotating shaft requires special precautions to prevent blockages. These blockage issues will cause high maintenance and limit the injection rate of the flux thus reducing productivity.

As a solution to these issues, Foseco developed the MTS 1500^[4], a robust blockage-free and reliable system to achieve multiple functions in a foundry including:

- Faster degassing using more efficient XSR / FDR rotor designs
- Cheaper cleaning & dressing especially in high-pressure die-casting
- Constant and repeatable sodium modification^{[5][6]}
- Cost efficient Ti-B grain refinement in gravity and wheels
- Cost saving for dressing in Aluminium HPDC
- Oxide removal in Aluminium HPDC, pistons, wheels and chip melting.

IMPROVED GRAIN REFINING IN LPDC WHEELS USING A NOVEL FLUX GRAIN REFINER

Aluminium wheels are one of the most important automotive castings made (mostly) using the Low-pressure diecasting process. As OEM wheels are considered safety components, it is critical for wheel castings to:

- be exempt of gas and shrinkage porosity
- be free of oxides and inclusions
- have a very fine microstructure which will ensure adequate mechanical properties

Grain refining^[7] is one of the critical steps which most foundries achieve by adding Ti-B rod master alloy. The typical addition rate is usually around 0.1%.

Table 1 details the key process parameters used in an Asian LPDC wheel foundry where A356 alloy is being treated in 700 Kg transfer ladle prior to transfer into the low-pressure furnaces.

Alloy A356.2	Ti-B traditional process	COVERAL* MTS 1582
Ladle Size	700 Kg	700 Kg
Ti-B Flux Quantity	-	310 g
Master alloy Ti-B rod	500 g	-
Degassing Time	9 min	9 min

Table 1. Key process parameters used in an Asian LPDC wheel foundry

This wheel foundry is using 500 g of Ti-B rod master alloy in their traditional process in order to achieve the required mechanical properties. The newly introduced Flux Grain refiner (COVERAL* MTS 1582)^[7] was able to achieve similar quality levels with only 310 g of flux addition.

Table 2 compares the degassing efficiency and titanium levels obtained with Ti-B master alloy and the novel grain refiner, COVERAL MTS 1582.

Alloy A356.2	Ti-B traditional process	COVERAL MTS 1582	Remarks
RPT Density @ 80mbar	2.65	2.65	Identical
Chemical Analysis	Ti: 0.114%	Ti: 0.114%	Same level
DAS in spoke section	45.88 μm	47.21 μm	Spoke section (Hot area)
DAS in rim section	26.09 μm	27.26 μm	Rim section (Cold area)

Table 2. Degassing efficiency and titanium level comparison

Furthermore, to compare both grain refining processes, the foundry took samples from wheels in order to measure UTS and Elongation.

Table 3 shows a clear improvement of the mechanical properties despite addition of a smaller amount of the novel COVERAL MTS 1582 grain refiner.

Properties in Wheel Hub	Ti-B traditional process	COVERAL MTS 1582
Yield Strength (N/mm^2)	208.1	213.5
Tensile Strength (N/mm^2)	276.0	286.7
Elongation (%)	6.8	8.0

Table 3. Improvement in mechanical properties

Figure 1 shows some micrography pictures taken from the wheel spoke which was treated with the novel COVERAL MTS 1582 grain refiner.^[7]

We can see that the structure is very fine and homogeneous, which is suitable for modern OEM wheels.

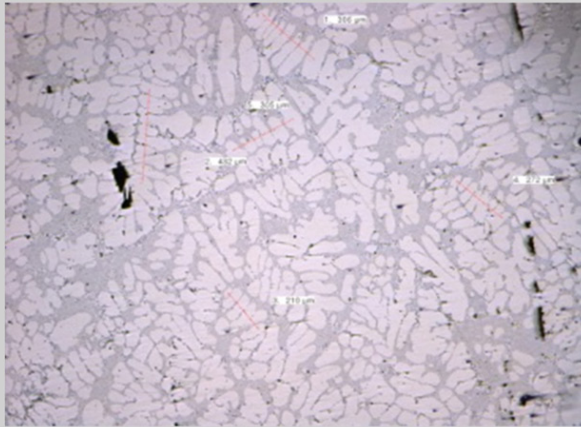
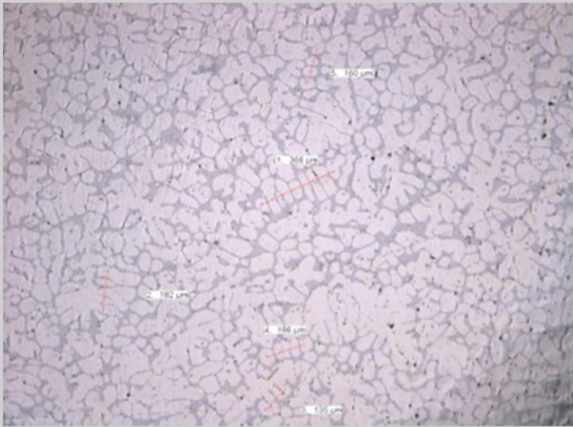
	Ti-B rod master alloy	Coveral MTS 1582 flux
Wheel Spoke	 <p>DAS = 45.88 μm</p>	 <p>DAS = 47.21 μm</p>
	The grain size has non-homogeneous areas	The grain size is very homogeneous.

Figure 1. Micrography comparison from wheel spoke

COST SAVING IN HPDC LADLE DROSSING USING MTS 1500 PROCESS

Drossing is a key part of ladle treatment in Aluminium foundries. Globally, more than 50% of all aluminium castings are now made using the High-Pressure diecasting process.

Metal treatment is usually carried out in transfer ladles using simple degassers for 3 – 5 min.

The purpose is not to degas the melt but to remove unwanted oxides and inclusions which will float up into the dross. These oxide films can lead to defects and casting failures.

HPDC creates huge amounts of aluminium dross which can be very rich in metallic Al droplets trapped within the dross.

Figure 2 shows the dross that was collected and sampled in a very large HPDC foundry making automotive castings. The standard dross is wet and heavy with trapped Aluminium.

While the dross collected after MTS 1500 is much lighter and poor in Aluminium. Dross samples were sent to our EN R&D laboratory which analysed residual Al metal in the dross using a salt melting technique which is common in the industry.

Table 4 shows the process comparisons between the foundry's current practice and our MTS 1500. It was found that this foundry can save up to 130 Tonnes of aluminium / year which represents an annual saving of at least USD 250 K. This foundry invested into 2 MTS 1500 units type Rotostativ in 2019. Additional units are being considered for the future.



Figure 2. Dross that was collected and sampled in a very large HPDC foundry making automotive castings

Automotive HPDC foundry	Standard HPDC process	New MTS 1500 process
Ladle capacity (Kg)	1400	1400
Collected dross quantity (Kg)	4.7	3.5
Aluminium content (%)	86.4%	43.6%
Aluminium lost in dross (Kg)	4.06	1.53
Aluminium saved / ladle (Kg)	-	2.53
Number ladles / day	180	180
Number ladles / year	54 000	54 000
Aluminium saved / year (Kg)	-	136 879
Flux cost / year (USD)	-	\$47 250
Foundry savings @ LME price	-	\$253 884

Table 4. Process cost comparison in HPDC

VMET ^[8] ASSESSMENT IN EUROPEAN WHEEL FOUNDRY

In the Last 20 years, aluminium wheels have become the standard for car makers around the world.

The preferred manufacturing route for OEM wheels is Low Pressure Diecasting (LPDC) using A356 alloy which can meet the required mechanical specifications after T6 heat treatment.

But adequate melt quality is a key requirement which can often be tarnished by the excessive presence of porosity, shrinkage, or oxides.

Some European wheel foundries asked us to conduct a melt quality audit using VMET to assess the quality of their melts. Samples were taken from their transfer ladles prior to (as melted) and after various treatment processes.

Table 5 summarizes the VMET findings and clearly shows significant quality improvements as:

- The total number of features is reduced by 93% after MTS 1500 (from 917 to 62).
- Total aluminium oxides is reduced by 93% after MTS 1500 (from 225 to 16)
- Other inclusions are reduced by 91% after MTS 1500 (from 92 to 8)
- More importantly, all the worrying features > 15 microns are reduced by 98% (from 137 to 3).

Foundry	VMET Features explanation	European Aluminium Wheel foundry		
Alloy		Al-Si7%-Mg0,3% (A356)		
Sample Description		A356 alloy as melted	After 10 min Rotary degassing (FDU)	After 10 min MTS 1500 treatment
Total Features	Total # of defects porosity & inclusions	917	377	62
Features by Nature & Chemistry				
Pore	Gas and shrinkage porosity	600	234	38
Aluminium Oxides (Al ₂ O ₃)	Aluminium Oxide & Mg Spinels	225	98	16
Other inclusions	Other inclusions (carbides, refractory, ..	92	45	8
Features and inclusions By Size				
0.50 – 15.0 µm	Little significance in castings	780	368	59
Σ all features > 15.0 µm	Defects are a concern in castings	137	9	3

Table 5. VMET analysis in a European wheel foundry

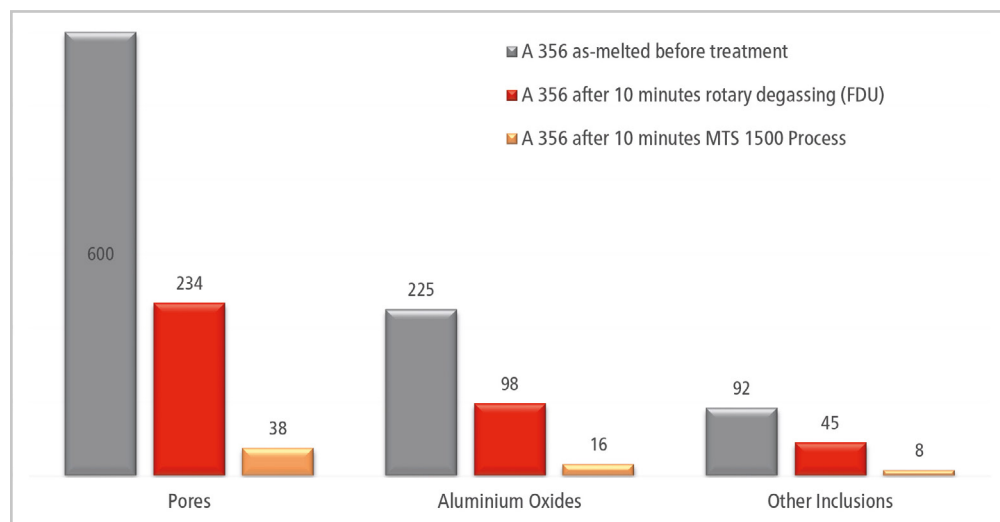


Figure 3. VMET in wheel foundry

VMET analysis is showing that MTS 1500 has a significant impact on melt quality in wheel foundries by reducing unwanted defects like porosity, oxides and other non-metallic inclusions as shown in Figure 3. This trend has led to a strong development of MTS 1500 use in wheel foundries around the world.

VMET ^[8] ASSESSMENT OF INTERMETALLIC INCLUSIONS IN HPDC FOUNDRY

More than 50% of all Aluminium castings are now made using the High-Pressure diecasting process in the world.

Metal is usually transferred from the melting to the casting furnaces using transfer ladles with capacities ranging from 300 Kg up to 1500 Kg.

During this melt transfer, some basic metal treatment is performed using rotary degassers for 3 – 5 min.

The purpose is not to remove hydrogen but unwanted oxide films and inclusions that can lead to defects and casting failures.

Figure 4 shows a typical transfer ladle undergoing metal treatment using MTS 1500 Rotostativ with following attributes:

- Casting: Automotive transmission
- Alloy: ADC12 secondary ingot
- Ladle capacity: 1400 Kg
- Flux addition: 0.03% COVERAL MTS 1565
- Treatment time: 3 min only
- Rotor XSR 220.70 + DSK 75/800.70

This automotive foundry asked to evaluate their melt treatment practice using VMET on several transfer ladles prior to filling the casting furnace. Table 6 shows the VMET results before and after MTS 1500 treatment in the transfer ladle.



Figure 4. MTS treatment in HPDC foundry

In the case of both ladles, the VMET analysis found:

- an overall reduction of the total number of features, oxides and inclusions.
- the oxides and inclusions larger than 15 μm were completely eliminated
- the Fe-linked intermetallic components that can be present in HPDC alloys were reduced significantly.

VMET shows a clear impact of MTS 1500 process on melt quality in HPDC.

Ladle	Ladle 1		Ladle 2		Comments/Explanation
	Before	After	Before	After	
Sample from ladle	Before	After	Before	After	
RPT density (g/cc)	2.27	2.62	2.25	2.61	Fit for purpose degassing improvement
Total Features	1973	296	243	70	Overall reduction of total features
Total aluminium oxides	1683	253	205	63	Overall reduction of oxide presence
0.5 - 15 μm	1682	253	205	63	Little significance in casting
> 15 μm	1	0	0	0	Reduction of oxides
Total other inclusions	290	43	184	7	Overall reduction of inclusions
0.5 - 15 μm	285	43	183	7	Little significance in castings
> 15 μm	5	0	1	0	Reduction of inclusions

Table 6. VMET results before and after MTS 1500 treatment

VMET^[8] ASSESSMENT OF MAGNESIUM OXIDES IN A PISTON FOUNDRY

Aluminium Pistons have become the norm in the automotive industry due to their relative strength vs light weight. But to achieve such performance, pistons must be free of porosity, oxides & inclusions as well as unwanted alkali elements like Na or Ca which at levels > 5 ppm will affect mechanical properties. One additional issue are the magnesium oxides forming in the melt due to the high Mg content of eutectic piston alloys like ACA8-336-LM13.

Hence, particular care is given to metal treatment which includes the use of rotary degassers with injection or addition of various fluxes or gases designed to remove such impurities. Chlorine gas (Cl_2) or chlorine releasing fluxes (C_2Cl_6) are still used in some parts of the world, but they are no longer perceived as the most environmentally friendly technology. As can be seen below, there are often strong chlorine emissions linked with the use of such toxic additives.

- $\text{C}_2\text{Cl}_6 + [\text{Na}] \rightarrow \text{NaCl} + \text{Cl}_2 \text{ gas}$
- $\text{C}_2\text{Cl}_6 + [\text{Ca}] \rightarrow \text{CaCl}_2 + \text{Cl}_2 \text{ gas}$

Due to environmental pressure, a new MTS 1500 technology shown in figure 5 has developed in Aluminium pistons foundries which combines the use of Rotary degassing using inert gases (Ar , N_2) and several types of fluxes which have dual functions:

1. remove oxides and especially MgO (spinel) which are a known problem in pistons
2. reduce all alkali elements like Na & Ca below 5 ppm

COVERAL MTS 1565 has been proven to effectively remove oxides and particularly MgO spinel inclusions in an environmentally acceptable manner.

COVERAL MTS 1591 can effectively remove unwanted alkalis according to the following mechanism: Coveral MTS 1591 + $[\text{Na}] + [\text{Ca}] \rightarrow \text{NaCl} + \text{CaCl}_2$ (which will float into the dross)

A market leading automotive piston foundry has asked us to use VMET to investigate their melt quality following a customer complaint linked to MgO inclusions.

Table 7 shows the VMET report and findings before and after metal treatment.



Figure 5. MTS treatment in a piston foundry

This VMET analysis was able to identify the presence of:

- excessive amounts of Na & Ca in the melt before treatment
- many small oxides and inclusions in the melt prior to rotary degassing treatment
- 26 MgO spinel inclusions in the sample, smaller than $15\mu\text{m}$
- 3 MgO spinel were found to be larger than $15\mu\text{m}$ = a real problem for pistons

VMET also showed that MTS 1500 process together with COVERAL MTS 1565 cleaning flux was able to significantly improve melt quality by removing all oxides and MgO inclusions > $15\mu\text{m}$.

This VMET work led to the sales of several MTS 1500 units in this piston foundry.

Piston Foundry	MTS 1500 Process with COVERAL MTS 1591/1565		
Trial	500 Kg Crucible		
Sample location	Before	After	Explanation
Na (ppm)	4	0.1	Excellent Alkali removal
Ca (ppm)	7.9	2.6	Excellent Alkali removal
Density Index (%)	7.5	0.1	Fantastic degassing performance
Total Aluminum Oxides	64	200	
0.5 – 15 µm	64	200	Breaking up of clusters - not a concern
Σ all oxides > 15 µm	0	0	No oxides found
Total Other Inclusions	69	74	
0.5 – 15 µm	66	74	Breaking up of clusters - not a concern
Σ all inclusions > 15 µm	3	0	Reduction of inclusions
Total MgO & Spinel	29	5	
0.5 – 15 µm	26	5	Reduction of spinels
Σ all MgO > 15 µm	3	0	Reduction of spinels

Table 7. VMET report and findings before and after metal treatment

VMET [8] ASSESSMENT OF CHIP MELTING OPERATION FOR FOUNDRY INGOT PRODUCTION

In recent years, many operations have looked at remelting machining chips in order to produce secondary ingots suitable for aluminium casting production. This is particularly true in Asia when very large amounts of A356 chips are coming from LPDC wheel machining.

But many such operations encounter quality issues as they underestimate the level of oxides created during the remelting of such finely divided chips which have large specific surfaces.

Hence extreme oxidation will create millions of very fine oxide films as shown in figure 6 where VMET found extremely high levels of oxide between 0.5 µm – 15 µm.

Such high levels of oxides will create excessive dross during melting but also aggregate to form larger oxide clusters & films which are the cause of reject castings.

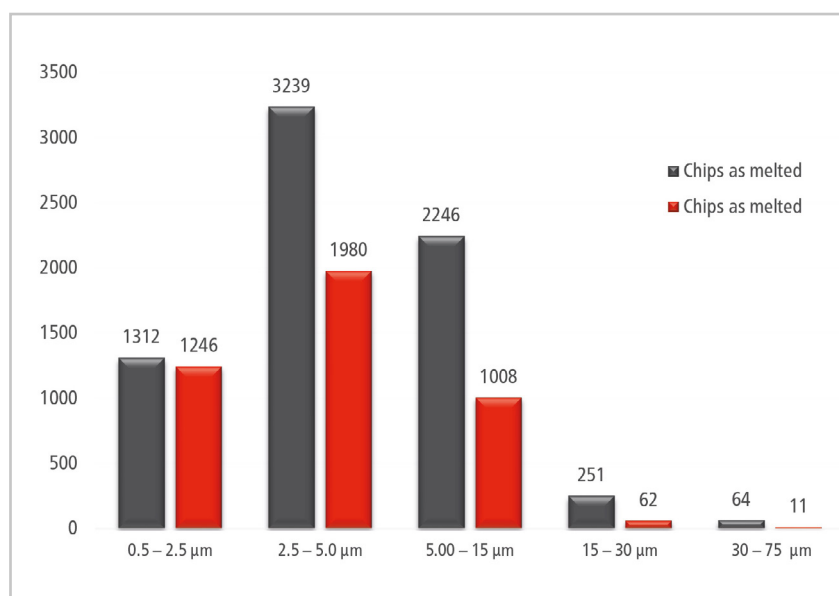


Figure 6. Features in Chip melts by size

Such chip generated melts must undergo intense metal treatment in order to reduce the level of oxides significantly. Strong cleaning fluxes should be applied to de-wet the oxide films and make sure they can be floated into the dross.

One secondary ingot maker asked us to implement such a metal treatment and use VMET to quantify the level of oxides and the improvement observed.

Figure 7 shows MTS 1500 on the fuel fired crucible furnaces that are used to remelt the 100% charges of A356 chips. The melting temperature exceeds 780°C. Foseco implemented a specially designed MTS 1500 type Mark 10 able to treat such chip melting furnaces.

VMET Samples were taken from one chip melting furnace before and after a 10 min MTS 1500 treatment. The SEM pictures with 100x magnification are shown in figure 8 below.

We can see the melt “as melted” shows many defects which are a mixtures of porosity and oxide films. Whereas after the 10 min MTS 1500 treatment, the sample is clean without any visible traces of oxides. This is a visual confirmation that MTS 1500 process is able to achieve good melt quality even with 100% pure melted chips.



Figure 7. MTS 1500 on the fuel fired crucible furnaces used to remelt the 100% charges of A356 chips

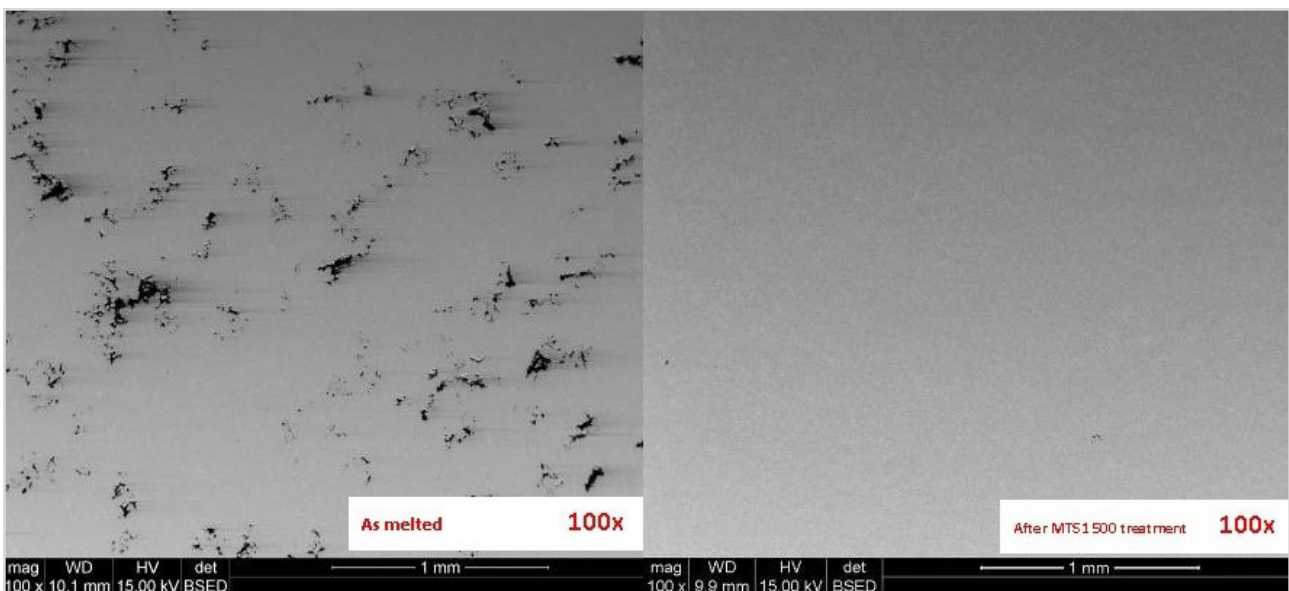


Figure 8. SEM pictures with 100x magnification

Two furnaces 1 & 2 (Table 8) with similar capacity were loaded with the same amount of chips. After a melting time of around 1 hour, the MTS 1500 unit was applied respectively to furnace 1 for 15 min and furnace 2 for 10 min.

All other working parameters were kept identical including:

- Furnace capacity: 750 Kg chips
- Gas flow: 20 l/min
- Flux addition: 1.2 kg (0.16%)
- Rotor Size: XSR Ø 220 mm
- Shaft length: 900 mm
- Treatment temperature: 720°C

The VMET data in table 8, clearly shows that the MTS 1500 treatment was able to significantly reduce most defects especially:

- Total # of features were reduced by 99% after a 10 min MTS 1500 treatment (4307 to 53)
- Total # of pores were reduced by 99% after a 10 min MTS 1500 treatment (3791 to 29)
- Total # of oxides were reduced by 94% after a 10 min MTS 1500 treatment (329 to 19)
- Total # of inclusions were reduced by 97% after a 10 min MTS 1500 treatment (187 to 5)

From this chip melting study, we can conclude that the MTS 1500 process is able to remove more than 98% of all defects in Aluminium melts treated in such crucibles.

Chip Melting	Furnace 1		Furnace 2	
Sample location	Chips as melted	After 15 min MTS	Chips as melted	After 10 min MTS
Total Features	7116	73	4307	53
Total Pores	3804	63	3791	29
Aluminium Oxides	2958	3	329	19
Other Inclusions	354	7	187	5
0.5 - 2.5 µm	1312	9	1246	17
2.5 - 5.0 µm	3239	21	1980	18
5.00 - 15 µm	2216	21	1008	11
15 - 30 µm	251	19	62	3
30 - 75 µm	64	2	11	4
> 75 µm	4	1	0	0

Table 8. VMET results before and after MTS when melting chips

CONCLUSIONS

Metal treatment is one of the critical parts of the foundry process, which often has a significant impact on casting quality, reject rates and costs. Existing practice may have limitations in terms of quality, efficiency or automation.

The MTS 1500 process clearly demonstrated higher degassing performance and better grain refining efficiency in low-pressure die casting wheels.

In high pressure die casting, MTS 1500 showed significant cost savings in terms of reduced dross generation.

MTS 1500 combined with VMET (Melt Quality Assessment) has clearly proven that it can significantly improve melt quality of Aluminium pistons, wheels, and chip melting, by significantly reducing detrimental oxides and inclusions.

REFERENCES

1. J. Campbell. Castings. Butterworth Heinemann, 2003.
2. Geoffrey K. Sigworth, Understanding Quality in Aluminum Castings.
3. J.G. Kaufman and E.L. Rooy, "Aluminum Alloy Castings", AFS (2005).
4. Philippe Kientzler, Jun Pascual, "MTS 1500 - A robust (blockage-free), reliable, environmentally friendly, lower cost Metal Treatment Station for Aluminium Foundries", 11th Asian Foundry Congress, Guangzhou, November 12th -15th 2011.
5. J.E. Gruzleski, "Treatment of Al-Si Alloys", AFS (1990).
6. M. Timpel et al., Acta Mat., vol.60, p3920 (2012).
7. J. Stonesifer, B. Began, Degassing and Flux Grain Refining in a Continuous Well at Littlestown Foundry, 2019 AFS Proceedings of the 123rd Metalcasting Congress, Atlanta, Georgia, USA, Paper 19-015.
8. Wenwu Shi, Vmet Analysis of Cast Aluminum Alloys, Fundamental, Application, and Statistic Analysis, AFS Conference on high integrity aluminum castings, October 5-7, 2015 Nashville, TN

CONTACT



PHILIPPE KIENTZLER

INTERNATIONAL MARKETING
MANAGER NON-FERROUS

philippe.kientzler@vesuvius.com
+81 080 2474 4161



TENCO XUE

PRODUCT GROUP MANAGER -
NON FERROUS

tenco.xue@vesuvius.com
+86 139 1836 7830



TAKEHIKO OKAMOTO

PRODUCT MANAGER,
NON FERROUS PRODUCTS

takehiko.okamoto@vesuvius.com
+81 90 5156 9233



PRAMUK UHAPATTANAPANICH

SALES MANAGER,
FOSECO (THAILAND) LTD

u.pramuk@vesuvius.com
+66 81822 0645



RECLAMATION OF INORGANIC BONDED SAND SYSTEMS TOWARDS A MORE SUSTAINABLE CORE PRODUCTION PROCESS



Authors: Dr. Vincent Haanappel and Thomas Linke, Foseco and Markus Jendrock and Dr. Enno Schulte, KLEIN Anlagenbau AG

An increasing number of automotive aluminum foundries are replacing organic with inorganic binder systems in order to reduce emissions of volatile organic compounds and ensure a more sustainable production process. If an efficient sand reclamation process for inorganic-bonded sand were developed, it would provide further benefits in terms of reduced emissions and energy consumption. This study presents an innovative process for reclaiming inorganic-bonded foundry sand, based on a mechanically-adsorptive process known as the CLUSTREG process. Results show that, even after 10 reclamation cycles, foundry sand derived from cores bonded with SOLOSIL* TX inorganic binder systems could be re-used, without detrimentally affecting the flowability of the sand mixture, or the mechanical properties and gas permeability of the manufactured cores. Although the pH value and conductivity did significantly increase after one reclamation cycle, this had no negative impact on the core quality of reclaimed sand.

INTRODUCTION

It is common knowledge that a large number of castings are manufactured in clay-bonded moulding materials [1]. For technical and economic reasons, the bentonite- or clay-bonded sand is now treated after use, with the result that most of the material can be re-used, reducing costs and environmental impact. This process is known as reclamation.

Separate to the above-mentioned clay-bonded sand systems, there is a large variety of organic binder systems for core and mould production [2]. These materials can also be reclaimed, using mechanical and thermal processes. The resin- or organic-bonded sand undergoes thermal exposure during casting and cooling, before the core residue is removed using a shake-out process. Some of the binder bridges close to the casting surface are exposed to high temperatures and are almost completely decomposed, which makes the shake-out less complicated. During mechanical reclamation, the binder can be relatively easily removed from the surface of the sand grains, as the strength of the organic binder bridges is quite low.

When using organic-bonded sand systems, emissions are mainly caused by burning off the organic binder components in the sand moulds or cores during the casting process. An increasing number of automotive aluminium foundries are therefore replacing organic with inorganic binder systems to reduce emissions of these volatile organic compounds, and to ensure a more sustainable production process [3]. If an efficient sand reclamation process for inorganic-bonded (IOB) sand could be developed, it would reduce emissions and energy consumption further still. However, the reclamation process for inorganic-bonded sand is, from a technical point of view, very different to that being developed for organic-bonded sand systems.

Aluminium automotive foundries use core packages consisting of base cores, inlet, outlet cores and water-jacket cores. The system is known as a mono-system, because only one

binder system is used, with, if needed, two different grain sizes (distribution) of silica sand. During the foundry process, the core package faces mild thermal exposure only in certain areas, for example, the inlet, outlet cores and the water-jacket cores. As a result of the low thermal impact, some areas in the core package remain at room temperature, while other parts undergo very short thermal exposure at 500 °C, before rapidly cooling to 200 °C within approximately 30 minutes.

When using inorganic binder systems, the binder bridges are generally more rigid, with higher mechanical resistance, compared to organic binder bridges; indeed, the hardness of the cured inorganic binder is close to the hardness of silica. Based on the higher abrasion resistance of the cured binder, sand reclamation processes that comprise only grinding of the grains are not recommended.

This study focuses on the development of a sand reclamation process for SOLOSIL TX inorganic-bonded sand cores from an automotive foundry. After presenting the CLUSTREG sand reclamation process, results from 10 reclamation cycles will be highlighted, including sand characteristics (particle size [distribution], LOI, pH, conductivity), flowability of the sand mixture, bending strength values and gas permeability of the manufactured cores.

DESCRIPTION OF THE PROCESS FOR RECLAIMING INORGANIC-BONDED SAND

With the CLUSTREG process (Figure 1), KLEIN Anlagenbau AG (WO 2017/137113 A1, Method and Device for Regenerating Foundry Sand) has developed an innovative mechanically-adsorptive process for the reclamation of water glass-bonded foundry sand. The process comprises a sequence of three main steps.

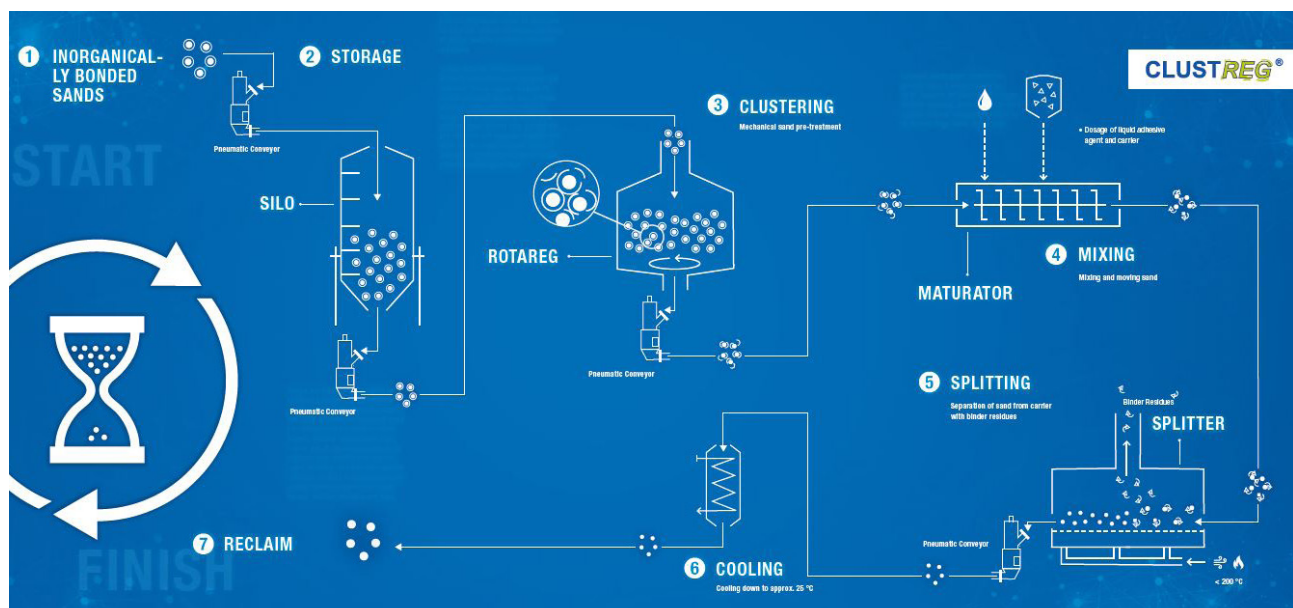


Figure 1. The CLUSTREG process

In the first step, the used sand is processed in a ROTAREG mechanical pre-cleaning unit (Figure 2). During this stage, the binder residues, additives and quartz dust (if present) are loosened from the sand grains and dedusted in a first dedusting stage. The used sand falls vertically from the top with a defined mass flow (10 t/h) to a rapidly rotating turntable. This accelerates the sand outwards and shoots it almost radially into a sand bed. The sand is cleaned by the impact and by rubbing the sand grains against each other. Depending on the desired degree of cleaning, the sand can circulate several times in the pre-cleaning unit. An initial pre-dedusting stage is integrated into the processing chamber.

After this mechanical treatment step, the sand is again intensively dedusted in a classifier. The main advantages of the ROTAREG are the gentle sand treatment, the robust and inexpensive plant technology and its ability to process many different binder systems, especially for water glass-bonded foundry sands.

In the innovative second step, the mechanically pre-treated sand is mixed with an adhesive agent and a carrier material in a specific way in a maturator. Binder residues and dust particles are bound to the carrier material in the used sand-adhesive agent-carrier mixture. The grain surface is also cleaned of fine dust particles. After the mixture has passed through the maturator, it enters the third treatment stage, the splitter.

In the splitter, the sand and the carrier material, now with the binder residues and dust components bound to it, are separated from each other. To do so, the mixture is passed over a fluidized bed, through which heated air ($< 200^{\circ}\text{C}$) flows from below. Due to the fluidization and specific suction, as well as the low density of the carrier material compared to the sand, the carrier material, binder residues and dust particles are discharged upwards and removed. After the sand has passed through the splitter, the regeneration process is complete and reclaimed sand can be re-used in the core making process.

During process development, great importance was attached to the fact that the plant technology is simple and robust and that, apart from the usual hardened wear parts required for sand treatment, no special materials are required (e.g., no heat-resistant steels, special sealing materials, etc.). It is also important to note that energy consumption is only about 20% of that of thermal reclamation plants for the reclamation of water glass-bonded foundry sands. Moreover, CLUSTREG plants are characterized by very encouraging regeneration results, including low sand loss.

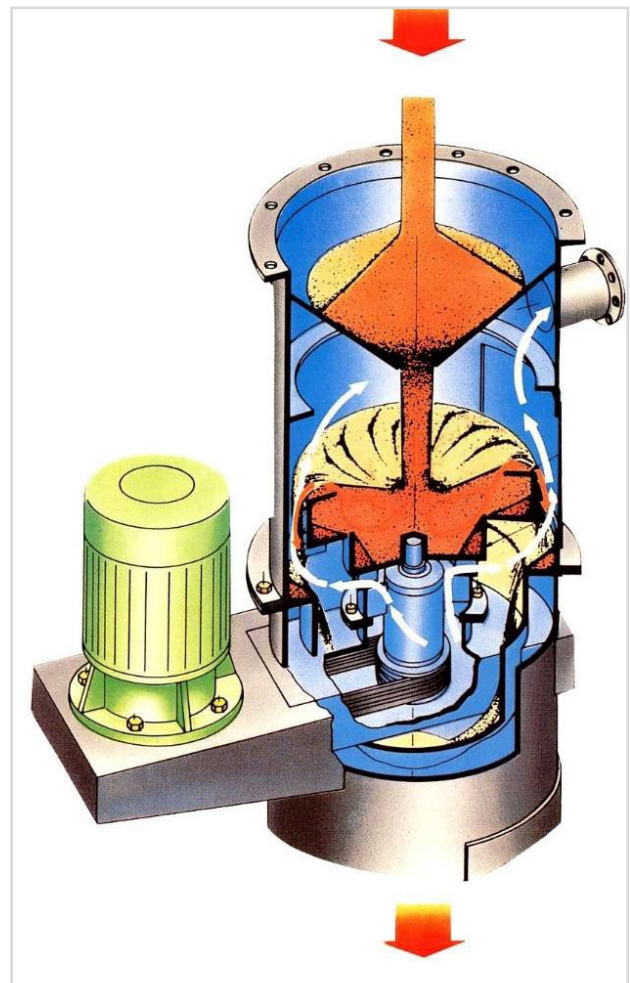


Figure 2. ROTAREG process principle, KLEIN Anlagenbau AG.

MATCHING PROCESSING PARAMETERS

For trials of the reclamation process, sand cores were manufactured on a Laempe core shooter. To provide a challenge, the sand cores were hot cured only, without any post-heat treatment. The process was carried out on inorganic-bonded sand cores with fully-developed mechanical strength.

As noted above, the process is characterised by various input parameters, which must be optimized to the type of inorganic-bonded sand cores. After some initial testing and analysis, including determining the optimized processing parameters, a first series of reclamation trials were started, each with 20 kg of used inorganic-bonded sand. During these cycles, the machine and processing parameters were kept constant.

METHODOLOGY AND RESULTS

In this section, several test methods will be presented and the results discussed in more detail. However, the intention is not to present all available results, which is beyond the scope of this paper, but to collect the most relevant data from the reclamation process for further managing sand systems in the foundry industry. As such, results from 10 reclamation cycles will be presented, including sand characteristics (particle size [distribution], LOI, pH, and conductivity), flowability of the sand mixture, flexural strength values, and gas permeability of the manufactured cores.

Sand characteristics

The starting point was a thermally-reclaimed organic-bonded sand based on LA32. Previous tests showed that the data / results of this thermally-treated sand are identical to new sand. Sand cores were manufactured using a Laempe-type core blower with additions of 1.70 wt% SOLOSIL TX (liquid binder) and 0.80 wt% SOLOSIL TX (additive); all percentages are based on sand. Table 1 lists the average particle size of the recycled sand together with the pH, conductivity and LOI values.

From this table, it can be seen that the particle size after reclamation was only slightly lower (AFS = 53-54) than the zero sample (i.e., the thermally-treated organic-bonded sand) with an AFS of 51.

More interesting were the pH and conductivity of the reclaimed sand. After the first reclamation cycle, the pH increased to values above 10, whereas the conductivity increased towards about 200 $\mu\text{S}/\text{cm}$. After two reclamation cycles, the pH was about 11, while conductivity increased towards values higher than 300 $\mu\text{S}/\text{cm}$. These high values can be explained by the use of an alkaline-type inorganic binder system, mainly based on sodium silicate. It is likely that a small amount of the binder residue remained present on the surface of the sand grains. There was however no negative impact on the strength data, as can be seen in Table 2. The LOI values remained relatively low, independent of the number of reclamation cycles, due to the use of the inorganic binder system.

As already mentioned, the particle size distribution was stable, without significant changes. Figure 3 shows micrographs of the sand after 0, 5 and 10 reclamation cycles. Interestingly, even after 10 cycles, the sand grains are still bright and shiny, an indication of the effectiveness of the sand reclamation process. It was found that the lower the brightness of the sand grains, the lower the mechanical strength and flowability of the sand mixture, which detrimentally affected the performance of the recycled sand. This can be observed from Figure 4, in which two batches are shown, the left part after maturation time 1 and the right part after maturation time 2, where maturation time 2 is less than maturation time 1.

Sample (cycli)	Av. Part. Size (AFS)	pH	Conductivity	LOI
00 – Foundry sand	272 μm (51)	6.1	4 $\mu\text{S}/\text{cm}$	0.18 %
01 – EN 1275	266 μm (52)	10.8	198 $\mu\text{S}/\text{cm}$	0.25 %
02 – EN 1305	260 μm (53)	10.8	358 $\mu\text{S}/\text{cm}$	0.22 %
03 – EN 1313	255 μm (54)	11.2	323 $\mu\text{S}/\text{cm}$	0.26 %
04 – EN 1317	254 μm (54)	11.0	326 $\mu\text{S}/\text{cm}$	0.28 %
05 – EN 1334	258 μm (54)	11.0	291 $\mu\text{S}/\text{cm}$	0.35 %
06 – EN 1478	262 μm (53)	11.4	372 $\mu\text{S}/\text{cm}$	0.34 %
07 – EN 1497	266 μm (52)	11.2	424 $\mu\text{S}/\text{cm}$	0.40 %
08 – EN 1531	263 μm (53)	11.6	438 $\mu\text{S}/\text{cm}$	0.41 %
09 – EN 1544	262 μm (53)	11.6	478 $\mu\text{S}/\text{cm}$	0.52 %
10 – EN 1578	253 μm (54)	11.0	417 $\mu\text{S}/\text{cm}$	0.42 %

Table 1. Average particle size, pH, conductivity and LOI as a function of the reclamation cycle. Foundry sand was always LA32.

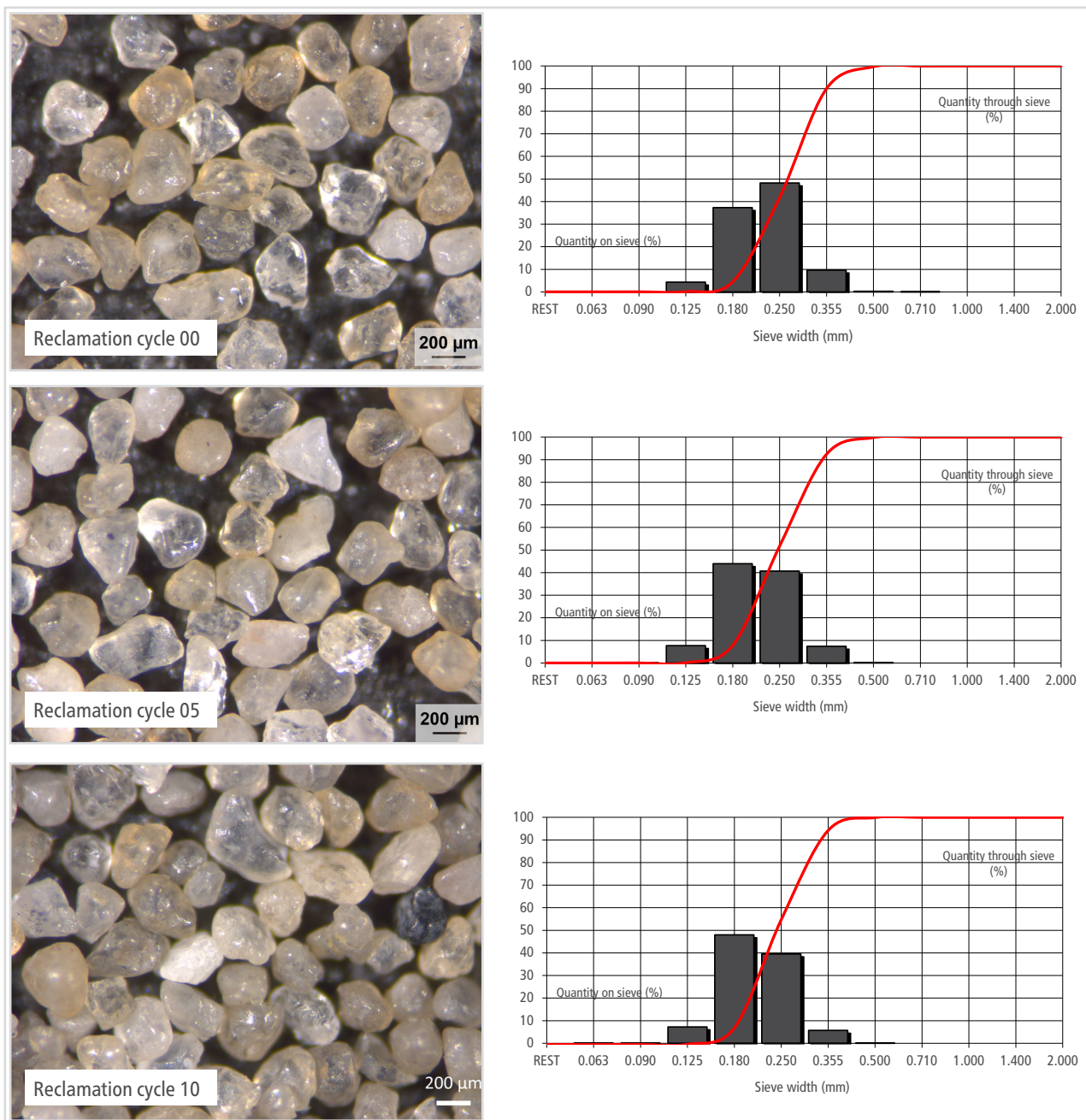


Figure 3. Microscope pictures of recycled sand, including grain size distribution. Top: after 0 cycles; middle: after 5 cycles; bottom: after 10 cycles.

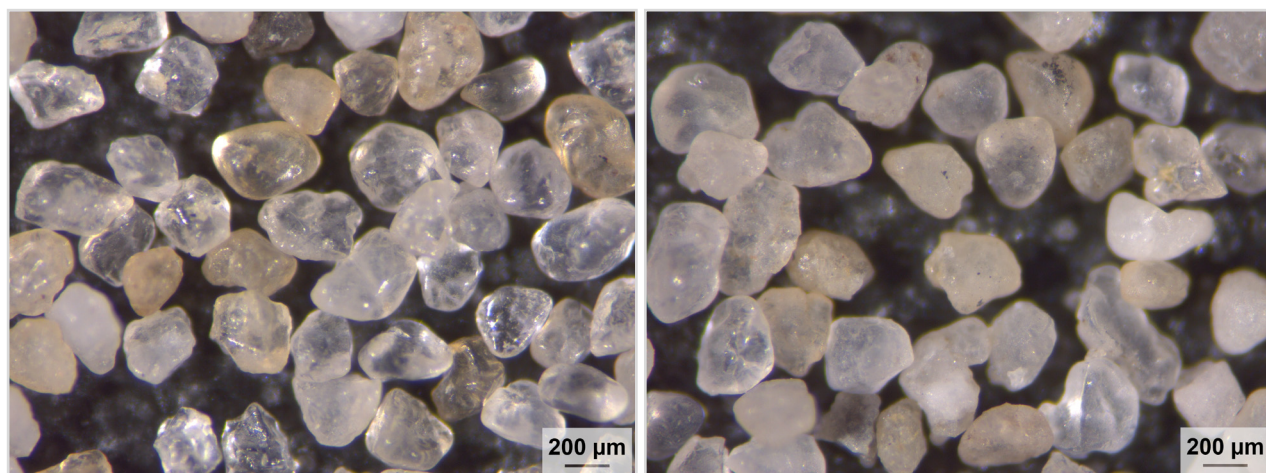


Figure 4. Appearance of sand grains: sample taken after maturation time 1 (left) and maturation time 2 (right) where maturation time 2 is less than maturation time 1.

Flowability

The flowability of the sand mixture was measured using a Brookfield Powder Flow Tester (PFT). This was initially developed to characterize the flow behavior of solid powder material with particle sizes up to a maximum of about 1 mm. As there was also a need to determine and to define the flowability of sand mixtures with a relatively small amount of a liquid, the PFT was used for these applications.

To compare different types of sand mixtures, the results are published in a flow function plot, as per Schulze [4]. This flow function plot shows the flowability of various types of samples over different 'consolidation stresses', these being considered as compressive stress. This plot shows various regions starting with free flowing and progressing through easy flowing, cohesive, very cohesive and non-flowing. The lower the curve, the higher the measured flowability. Figure 5 shows the unconfined failure strength (kPa) as a function of the major principal consolidating stress (kPa). Results from the sand mixtures show clearly that, irrespective of the number of reclamation cycles, under the highest compressive stress and in all cases, the sand mixture was easy flowing. The highest flowability was achieved with the zero-reclaimed sand mixture.

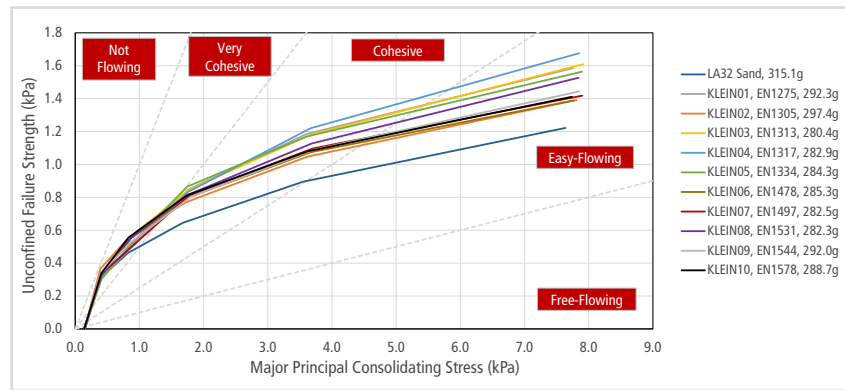


Figure 5. Flowability of sand mixtures after various reclamation cycles.

In relation to this, the weight of the sand mixture placed in the sample holder can also be an indirect indication of flowability.

In this case, the Hausner ratio [5] or the Carr index C [6] is sometimes used to obtain a more quantitative value of the flowability. The weight of the as-received sample (without reclamation) in this case was 315 g, while for the other sand mixtures, the weight was lower than 300 g, indicating slightly lower compaction, corresponding to slightly lower flowability.

Core characteristics

Table 2 lists the core weight, bending strength, flexural modulus and gas permeability as a function of the number of reclamation cycles. Measurements of the cores were done after 12 h storage at 25 °C and 30% RH.

This table clearly shows that the weight of the samples did not significantly change with the number of reclamation cycles and was always between 146 g and 143 g, indicative of compaction / good flowability of the sand mixture. Bending strength values started at 477 N/cm² (compared to a target value of 475 N/cm²) and increased slightly after reclamation. Irrespective of the number of reclamation cycles, strength values were always between 500 and 540 N/cm².

The reason for the slight increase in strength was the removal of fines during the process. The flexural modulus showed no relation to the number of reclamation cycles and was always between 4.1 and 5.4 Mpa. Gas permeability started to increase initially after reclamation but stabilized around 150 mD.

Sample (cycli)	Core weight	Bending strength	Flexural Modulus	Gas Permeability
00 – Foundry sand	145.6 ± 0.3 g	477 ± 7 N/cm ²	4.3 ± 0.4 Mpa	140 ± 1 mD
01 – EN 1275	144.7 ± 0.2 g	495 ± 2 N/cm ²	5.4 ± 0.1 Mpa	157 ± 3 mD
02 – EN 1305	144.7 ± 0.2 g	531 ± 12 N/cm ²	4.9 ± 0.1 Mpa	147 ± 2 mD
03 – EN 1313	142.5 ± 0.1 g	537 ± 18 N/cm ²	4.7 ± 0.1 Mpa	153 ± 4 mD
04 – EN 1317	142.6 ± 0.1 g	505 ± 11 N/cm ²	4.9 ± 0.1 Mpa	159 ± 2 mD
05 – EN 1334	142.6 ± 0.2 g	519 ± 9 N/cm ²	5.1 ± 0.2 Mpa	155 ± 1 mD
06 – EN 1478	143.9 ± 0.2 g	504 ± 11 N/cm ²	4.4 ± 0.1 Mpa	142 ± 1 mD
07 – EN 1497	142.8 ± 0.2 g	508 ± 17 N/cm ²	4.1 ± 0.2 Mpa	148 ± 1 mD
08 – EN 1531	143.6 ± 0.2 g	498 ± 5 N/cm ²	4.1 ± 0.1 Mpa	158 ± 1 mD
09 – EN 1544	144.3 ± 0.3 g	500 ± 23 N/cm ²	4.1 ± 0.2 Mpa	139 ± 1 mD
10 – EN 1578	143.8 ± 0.4 g	521 ± 32 N/cm ²	4.4 ± 0.1 Mpa	138 ± 2 mD

Table 2. Core weight, bending strength, flexural modulus and gas permeability as a function of the reclamation cycle. Foundry sand was always LA32.

SUMMARY

This study presents an innovative process for the reclamation of inorganic-bonded foundry sand, based on a mechanically-adsorptive process called the CLUSTREG process [7]. After pre-testing with different processing conditions to optimize the various processing parameters, 10 reclamation cycles were performed while maintaining constant machine parameters. Results from these 10 reclamation cycles are presented, including sand characteristics (particle size [distribution], LOI, pH, conductivity), flowability of the sand mixture, bending strength values and gas permeability of the manufactured cores. It was found that, even after 10 reclamation cycles, foundry sand derived from cores with inorganic binder systems could be re-used, without detrimentally affecting flowability of the sand mixture, and the mechanical properties and gas permeability of the manufactured cores. Although the pH and conductivity did increase significantly after one reclamation cycle, this had no negative impact on the core quality of reclaimed sand.

From these results, it can be concluded that, after starting with the most challenging parameters to stress the process and installation, and with the support of laboratory results to optimize the machine parameters, improved processing parameters could be determined. With this set of processing parameters, no issues occurred with this type of SOLOSIL TX inorganic-bonded sand after 10 reclamation cycles.

In future, a smaller project is planned to include five reclamation cycles with cores that will face a thermal load comparable to foundry conditions.

ACKNOWLEDGEMENT

The authors gratefully acknowledge Joachim Buchen Managing Director (KLEIN Anlagenbau AG, Freudenberg, Germany) and Tim Birch (Foseco UK, Tamworth, United Kingdom) for their contribution to this study.

Thanks are also due to J. Morsink (Foseco EN, Enschede, the Netherlands) for his contribution to the analysis and characterization of the samples.

REFERENCES

1. Limmaneevichitr, C., & Eidhed, W. 1. W.B. Parkes, Clay-bonded Foundry Sand, Applied Science Publishers, 1971 (ISBN: 0853345015, 9780853345015)
2. J. Brown, Foseco Foundryman's Handbook, Butterworth-Heinemann, 1994 (ISBN: 9780750619394)
3. H. Polzin, Anorganische Binder, Schiele & Schön, 2012 (ISBN: 9783794908240)
4. D. Schulze, Powders and Bulk Solids - Behavior, Characterization, Storage and Flow, Springer (2007).
5. R.E. Riley, and H.H. Hausner, Effect of particle size distribution on the friction in a powder mass, Int. J. Powder Met., 6 (1), 1970, pp. 17-22.
6. J. Cain, An alternative technique for determining ANSI/CEMA standard 550 flowability ratings for granular materials, Powder Hand. Proc., 14 (3), 2002, pp. 218-220.
7. E. Schulte, Klein AG, Deutscher Gießereitag Magdeburg 2016

CONTACT



THOMAS LINKE

International Project Manager
Mould & Core

thomas.linke@vesuvius.com
+31 53 751 5091



PARADIGM SHIFT: AN INDIAN FOUNDRY EXPERIENCE



Authors:

Archis Patankar, Manilal Bhimani and Sondip Bor, Foseco India Limited and
Paramasivan Subramanian and Rajkumar B, Bradken India Private Limited

Bradken and Foseco are two leading global companies in their respective fields. In India, there has been a close association between these two organisations which is principally based on mutually rewarding partnership and working together on many value creating projects related to improvements in foundry processes and the development of castings.

The objective of this paper is to highlight the outcome of joint efforts between Foseco and Bradken and share the benefits of working together.

INTRODUCTION

Bradken and Foseco are two leading global companies in their respective fields. In India, there has been a close association between these two organisations which is principally based on mutually rewarding partnership and working together on many value creating projects related to improvements in foundry processes and the development of castings.

In the early part of 2019, during one of the joint meetings between Bradken and Foseco Management Teams, while discussing future global trends and casting quality requirements it was pondered how Bradken and Foseco could further work together to meet new challenges. As an outcome of the initial discussions, it was decided to work on the following two broad areas of foundry operations mainly addressing environmental concerns and to be cost competitive.

Coating:

- Overall quality enhancement in surface finish of castings
- Reduction in coating cost while maintaining the existing quality standards.

Feeding Systems:

- Improvement of Inventory Management
- Innovative packing methodology to avoid transit losses
- Development of new products to address special needs

Joint projects as above were specifically initiated since Bradken Management highlighted that in spite of present market situation, they have challenging targets considering improved production at Bradken India site with increased expectation with regards to maintaining high safety standards, delivering excellence in all operations, and continual focus on cost optimisation.

Once these specific requirements were understood a joint effort was invested which lead to many new initiatives. These included new sleeve designs,

new packaging methods and the INSTA concept in coating which delivered significant benefits in overall coating process, achieving all the objectives set in the beginning.

The objective of this paper is to highlight the outcome of joint efforts of Foseco and Bradken and share the benefits of working together.

JOINT WORKING IN THE AREA OF COATINGS

In addition to improvements in surface finish and optimisation of coating cost, Bradken also showed interest to work on enhancement of their HSE norms in their foundry by eliminating or reducing the usage of plastic (packing material) in their foundry process.

Figures 1, 2 and 3 explain in brief the requirement of Bradken i.e. Focus on Safety, sustainable reduction in cost and process time with enhanced casting quality along with equal emphasis on environment aspects of foundry operations.

To summarize, the current challenges being faced by our partner and looking for improvements in areas like,

- Overall cost reduction
- Improve casting surface quality (finish)
- Minimized usage of plastic

Internally teams were formed at Foseco as well as in Bradken to investigate all aspects of coating preparation and application.

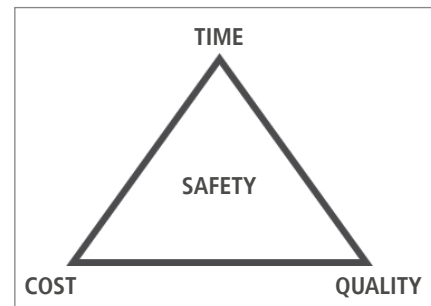


Figure 1. Project Objectives



Figure 2. Need of foundry industry – Go Green



Figure 3. Plastic wastage: a severe threat to society (Source: Study in science advances. The Economic times)

All these areas of improvements were discussed in detail with our R&D Teams and the discussion lead to the development of an innovative coating technology called INSTA*.

A proposal highlighting above benefits of INSTA TECHNOLOGY was presented to Bradken Management in the Month of May 2019.

After joint discussions and exchange of ideas between Foseco and Bradken teams it was decided jointly that INSTA technology should be assessed at Bradken Foundry.



STEPS FOLLOWED FOR INSTA PROJECT EXECUTION

1. Joint process mapping: Understand the existing practice, mould and core making, type of castings being made, metal grades, sand systems, core shop operation and identify location for equipment.
2. Understanding Bradken shop floor requirement with regards to coating operations: Every step was studied, including tests performed on as received coatings, coating preparation, adjusting to final application consistency, coating application, drying of coating, final finishing, closing practice and pouring.
3. Equipment support: New INSTA mixer was designed for high performance coating mixing and provided to Bradken as a part of INSTA TECHNOLOGY

WHAT IS INSTA?

- HOLCOTE* INSTA (A combination of refractory fillers, rheological conditioners & binder system)
- HOLCOTE INSTA, a single part refractory coating premix which delivers highly consistent coating when mixed with water.
- INSTA Mixer: Specifically developed for Bradken



Figure 4. INSTA coating and Mixer for coating preparation at Bradken

1. A highly accurate, consistent, efficient machine for preparation of INSTA coating.
2. Designed by Foseco with all safety features considering Bradken's Safety requirement.
3. Timer-controlled mixing with auto stop, RPM regulator and emergency control.

The benefits of INSTA coatings are:

1. reduced overall coating cost in use
2. elimination of plastic buckets
3. improved application consistency due to introduction of INSTA MIXER
4. consistent casting finish.

INSTA COATING: TRIALS

- HOLCOTE INSTA Coating
- Initial trial was conducted with preparation of a batch of 205 kg INSTA coating.
- Mixing ratio:
 - INSTA Coating: 125 kg
 - Water Addition: 80 Kg
 - Total outcome: 205 kg coatings ready for use
 - Coating Baume: 95 to 100 unit
 - % Dilution: 64 %
- Coating layer applied on mould: 3 layers
- Wet film thickness: 800 to 900 microns
- Coating drying: torching (Individual layer)
- Coating appearance: coverage and bond was found satisfactory.
- Trial casting weight: 4MT
- Mould and Core: Furan binder systems
- Pouring Temperature: 1560 Deg. C

Bradken management supported in joint evaluation of Trials, supported all the development work and provided their valuable inputs for executing INSTA project in "First Time Right" manner.

Through INSTA technology we could achieve much higher dilution (up to 65%) for INSTA coating and delivered superior casting quality compared to conventional coatings.

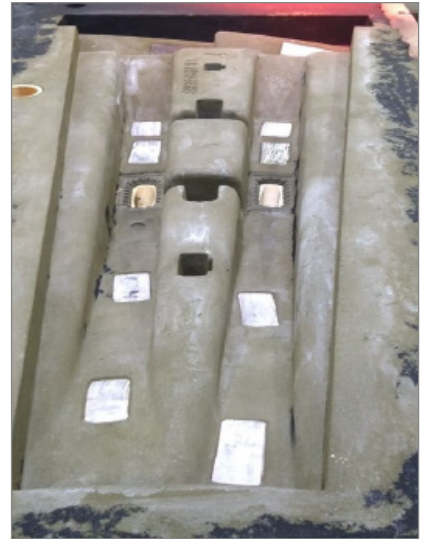


Figure 4a and b. Shows the mould/core before coating with INSTA coating.



Figure 5a and b. Mould/core coated with INSTA coating



Figure 6a and b. Casting results with HOLCOTE INSTA

BULK EVALUATION OF INSTA TECHNOLOGY

Based on Initial encouraging results, Bradken team decided to adopt INSTA technology on the shop floor.

At the time of publishing this paper, 30MT of INSTA coating used over a 6-month period has been successfully tested by Bradken.

BENEFITS TO BRADKEN THROUGH JOINT PROJECT OF INSTA TECHNOLOGY:

INSTA project aimed to deliver

- Savings in the coating cost as per initial estimation up to 15 %
- Consistent surface finish
- Elimination of HDPE buckets: which was one of the major SHE initiatives for Bradken

OUTCOME

Based on 6 months extended run with INSTA technology, this project delivered following benefits

- Eliminate usage and generation of plastic buckets.
- Improved application consistency due to introduction of equipment and consistent casting finish
- Delivered Cost saving up to 23% on existing coating consumptions- which is higher than the saving proposed to Bradken before commencement of project. Higher percent savings were mainly possible due to coating process optimization at Bradken.
- Going Forward: Introduction of palatized packing of INSTA coating for easy transportation and handling.



Figure 7. Palletised packing of INSTA coatings for easy handling at Foundry

JOINT WORKING IN AREA OF FEEDING SYSTEMS

Since 2018, Bradken India started ramping up its manufacturing, nearly doubling production volume. However, increased production also brought challenges with respect to Bradken casting metal grades which are non-repairable and large casting sizes.

In the area of Feeding systems, the challenges are:

- Inventory management considering of higher volumes of sleeves, varying in size and large numbers of sleeves being used.
- Consistent feeding performance leading to consistent casting quality.
- Easy removal of risers with minimum contact area, facilitating faster casting throughput with minimum fettling.

INVENTORY MANAGEMENT

At Bradken, with increased production volumes, it was a major challenge to maintain the optimum inventory of feeding system products. The issues faced were:

- Complex requirements of sleeves due to a higher number of sleeves in different sizes and types.
- Longer supply chain from the Foseco Plant to Bradken stores.
- Often leading to possible stock out situations causing production disruption.
- Also, at the same time we wanted to avoid excess inventory levels to avoid blocking space and capital.

In order to address the above points, a joint team was formed between Bradken and Foseco in order to understand the entire supply chain.

This team extensively studied all Feeding System process points including:

- Consumption pattern of each SKU
- Full process of stock movement & placing orders.
- Processing of orders and manufacturing planning at Foseco
- Actual manufacturing, testing and packaging
- Pattern of dispatch considering the way sleeves are loaded and unloaded in the trucks.

The above analysis helped in understanding importance of planning and execution of orders at Foseco based on Bradkens priorities and necessary actions were put in place. Improvements were required with regards to packing which would help to reduce transport losses.

Additionally, for improving overall efficiency a need was seen to develop customized shapes meeting Bradken's enhanced requirements.

IMPROVEMENT IN PACKING

Before this joint work, Foseco supplied sleeves in loose trays stacked one above each other. This, coupled with distances involved, occasionally resulted in considerable transit damage. In addition to the material loss involved in the transit, additional issues were caused by not having the right material available as per production schedules at Bradken which caused disruption and non-value-added work at both ends.

To overcome the problem, several options of packing were considered before focussing on a palletized packing method. This suggestion was immediately supported by Bradken and after initial assessment for effectiveness, it was employed as a permanent measure. This is shown in figure 8.

BENEFITS INVOLVED WITH PALLETISING

- About 5% reduction in transit losses due to breakage.
- Availability of right material on time. No production loss or need of last-minute changes.
- Overall reduction of non-value-added work on both sides avoiding any emergency management of the situation.

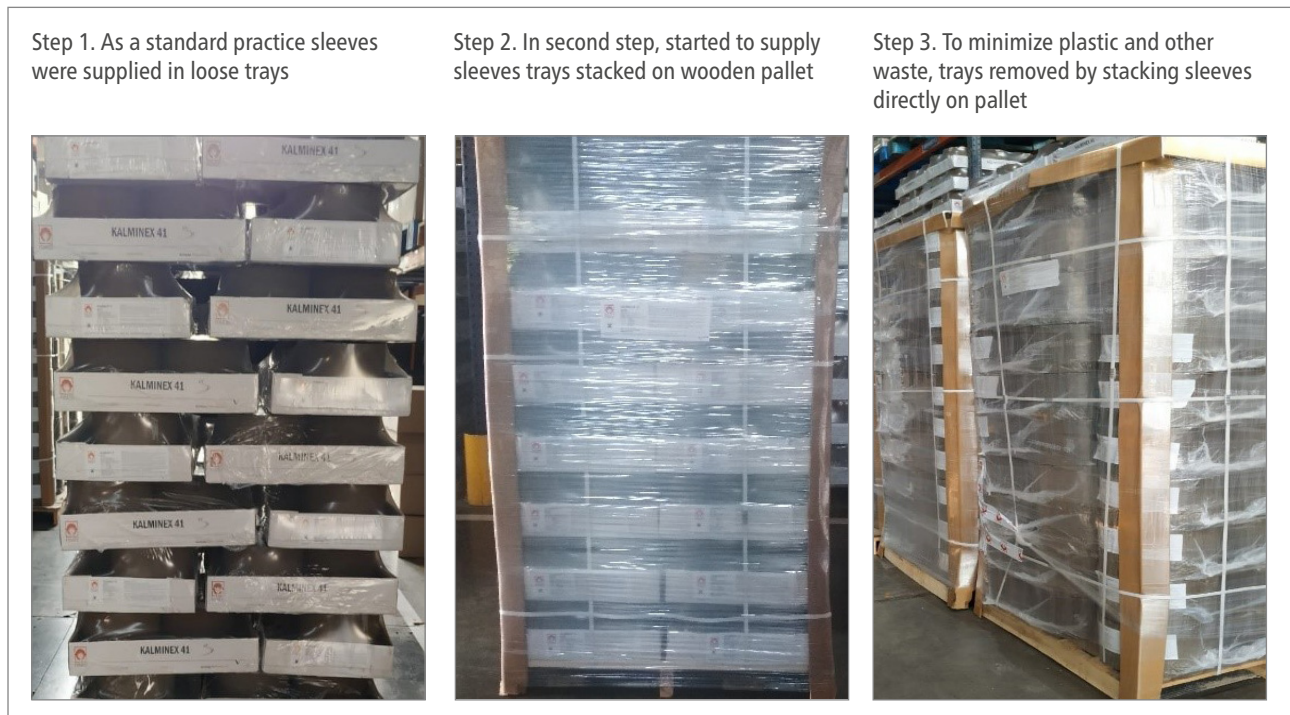


Figure 8. The progress of packing improvement initiative

DEVELOPMENT OF NEW PRODUCTS FOR BRADKEN'S REQUIREMENT

A. Slotted Neck Down sleeves

Application of standard Neck Down (ND) sleeves has been very common at Bradken resulting in many benefits:

- Ease of riser removal due to smaller contact area
- Substantially reduced riser neck grinding work.
- Ease of sleeve application where the casting contact area is limited.
- It helps to avoid sleeve projecting out and the need for a metal pad.
- Benefits of the ND sleeves were further extended by introducing "Slotted ND sleeves". Slotted ND sleeves facilitate application in specific casting geometries with minimum fettling work. (Figure 9)

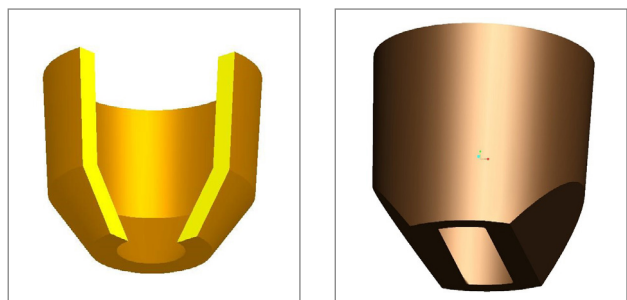


Figure 9. Standard (left) and Slotted (right) ND Sleeve design

B. Neck Down sleeves with Larger Neck Opening.

ND sleeves are designed with a neck opening as small as possible in order to gain the benefits associated with lower feeder contact area.

However, feeding behaviour of the casting metal during solidification is the main decisive factor to limit the opening of the neck.

To balance the sound feeding of casting during solidification and minimum neck opening, ND sleeves with different neck openings were designed specifically for Bradken. ND sleeves with 60% and 72% neck openings were introduced in addition to the 50% standard neck opening (figure 10).

The benefits of ND sleeves were further extended by introducing "Higher Neck opening ND sleeves" which facilitated effective feeding of metal grades that were typically difficult to feed through standard 50% neck opening ND Sleeves.

C. Kapex For Higher Size Sleeves

All ND sleeves and cylindrical sleeves above a 6" diameter are open sleeves. However, it is very common practice to make many open sleeves to perform like blind based on location of the sleeves by covering top face of open sleeves. Foundries normally cover the top sleeve face by sand cores, but this method certainly compromises the performance of blind feeders.

Foseco has a unique offering to such problems which are typically solved by using Foseco's innovative development named KAPEX* (figure 11). This helps to make open sleeves perform like a blind sleeve and ensure consistent performance of bigger feeders.

However, in the case at Bradken, the existing range of KAPEX was not enough and it required development of specific customized sizes. The KAPEX product range was expanded to cover additional sleeve sizes as per Bradkens requirement.

D. Sleeves With Customised Height

It is common practice in making heavier castings to build the required sleeve height by stacking another sleeve or cut piece of another sleeve on top.

Thus, often the sleeve height build up requires manual operation of sleeve cutting. To avoid this manual sleeve cutting operation required for additional height build up was analysed by Bradken and Foseco. A sleeve range (three customized sizes) with additional height was introduced to avoid manual cutting of sleeves resulting in improved productivity and ease of operations.

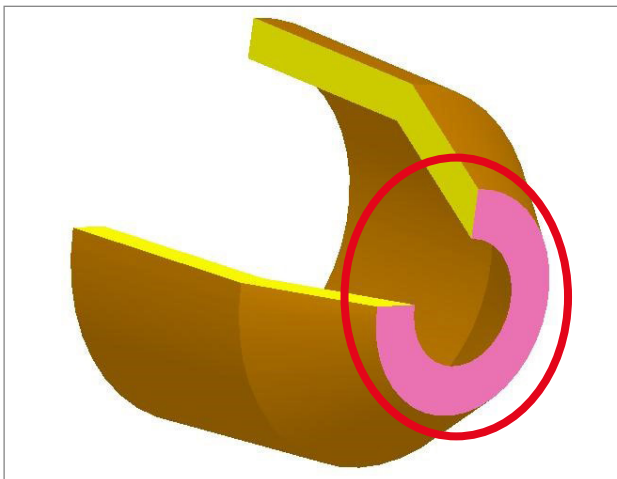


Figure 10. ND Sleeves with higher neck opening



Figure 11 . showing Typical "KAPEX"

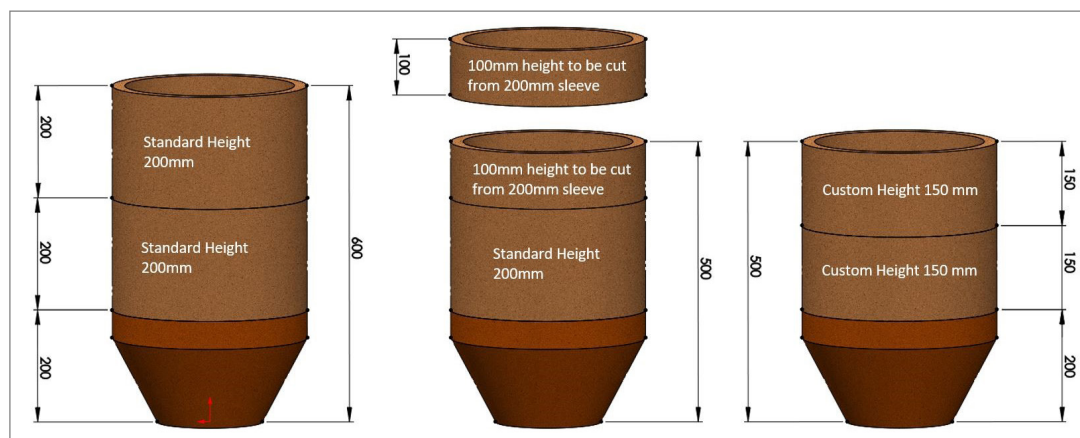


Figure 12. Sleeve with Customized height in Moulding

CONCLUSIONS

Foseco India and Bradken believe that working together in partnership is key to address current and future challenges.

The experience of working together on numerous initiatives ultimately lead to the following benefits through which enhanced foundry performance:

- Significant reduction in coating cost through implementation of INSTA.
- Introduction of process control equipment like the INSTA mixer helps to improve process consistency and deliver consistent coating application.
- Reduced transportation cost, reduced handling, and improved space availability at stores optimised inventory costs.
- Joint working and better understanding of each other's needs and capabilities, lead to the development of customised sleeves – which once implemented reduces rework, improves casting soundness and thus enabling faster casting throughput from fettling shops.
- Innovative approach like INSTA and improvement in packaging not only helps in achieving primary goals such as cost optimisation and inventory management but also helps in achieving environmental benefits by reducing the use of plastic from the process significantly.

REFERENCES

- Foundry Practice: Advance Coating Technology, N. Hodgkinson - Foseco Metallurgical Inc.
- Thorpe. (P J.), Avoidance of metal penetration and sand burn on in iron castings
- "Process to manufacture metals and alloys" H. Goldschmidt - German Patent Reference: DE 96 317 March 1895

ACKNOWLEDGEMENTS

The authors, gratefully acknowledge the collaboration and permission given from the management of Foseco India Limited and Bradken India Private Limited to present this paper.

CONTACT



ARCHIS PATANKAR

HEAD – MARKETING &
TECHNOLOGY

FOSECO INDIA LIMITED

Archis.patankar@vesuvius.com



MANILAL BHIMANI

SOLUTION MANGER -
METHODING

FOSECO INDIA LIMITED

manilal.bhimani@vesuvius.com



SONDIP BOR

SOLUTION MANAGER -
COATINGS

FOSECO INDIA LIMITED

sondip.bor@vesuvius.com

DISCOVER MORE

*Want more info about INSTA
Coating Technology?*

All rights reserved. No part of this publication may be reproduced, stored in a retrieval system of any nature or transmitted in any form or by any means, including photocopying and recording, without the written permission of the copyright holder.

All statements, information and data contained herein are published as a guide and although believed to be accurate and reliable (having regard to the manufacturer's practical experience) neither the manufacturer, licensor, seller nor publisher represents or warrants, expressly or impliedly:

- (1) their accuracy/reliability
- (2) that the use of the product(s) will not infringe third party rights
- (3) that no further safety measures are required to meet local legislation

The seller is not authorised to make representations nor contract on behalf of the manufacturer/licensor.
All sales by the manufacturer/seller are based on their respective conditions of sale available on request.

*Foseco, the logo, COVERAL, HOLCOTE, INSTA, KAPEX, SEDEX, SEMCO and SOLOSIL are Trade Marks of the Vesuvius Group, registered in certain countries, used under licence.

© Foseco International Ltd. 2021

CLUSTREG and ROTAREG are trademarks of KLEIN Anlagenbau AG.

COMMENT

Editorial policy is to highlight the latest Foseco products and technical developments. However, because of their newness, some developments may not be immediately available in your area.

Your local Foseco company or agent will be pleased to advise.



Foseco International Limited
P.O. Box 5516
Tamworth
Staffordshire
England B78 3XQ
Registered in England No. 468147

VESUVIUS